ANL-78-67

ANL-78-67

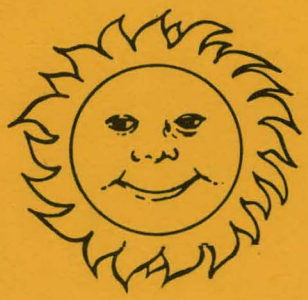

SIMPLE PROCEDURE FOR PREDICTING LONG-TERM AVERAGE PERFORMANCE OF NONCONCENTRATING AND OF CONCENTRATING SOLAR COLLECTORS

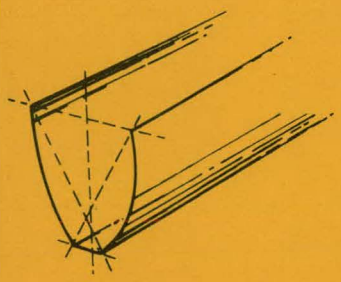

by

Manuel Collares-Pereira and Ari Rabl

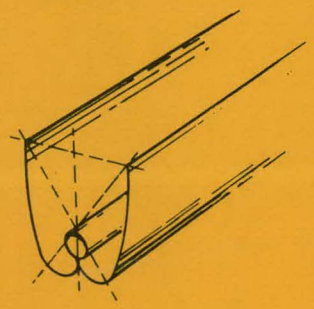

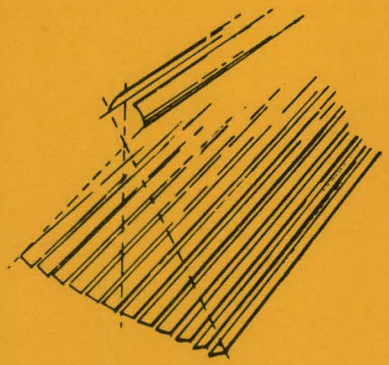

U of C-AUA-USDOE

ARGONNE NATIONAL LABORATORY, ARGONNE, ILLINOIS

Prepared for Solar Heating and Cooling
Research and Development Branch,
Conservation and Solar Applications,
U. S. Department of Energy
under Contract W-31-109-Eng-38

DISCLAIMER

Printed in the United States of America
Available from
National Technical Information Service
U. S. Department of Commerce
5285 Port Royal Road
Springfield, Virginia 22161
Price: Printed Copy $5.25; Microfiche $3.00

Distribution Category:
Solar Thermal (UC-62)

ANL-78-67

ARGONNE NATIONAL LABORATORY
9700 South Cass Avenue
Argonne, Illinois 60439

SIMPLE PROCEDURE FOR PREDICTING LONG-TERM AVERAGE PERFORMANCE OF NONCONCENTRATING AND OF CONCENTRATING SOLAR COLLECTORS

by

Manuel Collares-Pereira and Ari Rabl

June 1978

Work supported by the
Solar Heating and Cooling
Research and Development Branch,
Conservation and Solar Applications,
U. S. Department of Energy

THIS PAGE

WAS INTENTIONALLY

LEFT BLANK

TABLE OF CONTENTS

		Page
	ABSTRACT	ix
I.	Introduction	1
II.	Insolation $\bar{H}_{coll}$ Reaching Collector Aperture within Its Acceptance Angle	5
III.	Heat Loss, Utilizability, and Cutoff Time	11
IV.	Sample Calculation	16
V.	Comparison Studies	19
	A. One Axis (Polar) Tracking versus Two Axis Tracking	20
	B. Polar versus East-West Tracking Axis	20
	C. Flat Plate: Fixed versus Tracking	23
	D. Effect of Ground Reflectance	24
	E. Collection of Diffuse Radiation as Function of Concentration	25
	Acknowledgments	28
	References	29
	APPENDIX A: Extraterrestrial Insolation	32
	APPENDIX B: Long Term Average Values of Insolation, Clearness Index, and Ambient Temperature	33
	APPENDIX C: Specification of Instantaneous Efficiency	34
	Tables I to X	40
	Figures 1 to 7	53

LIST OF FIGURES

No.		Page
1.	$\bar{H}_d/\bar{H}_h$ versus $\bar{K}_h$ (Eq. II-3);	7
2.	Utilizability ϕ versus the critical ratio X for $\bar{K}_h$ = 0.7 and nine values of R from 0 to 0.8.	13
3.	Utilizability ϕ versus the critical ratio X for $\bar{K}_h$ = 0.6 and nine values of R from 0 to 0.8.	13
4.	Utilizability ϕ versus the critical ratio X for $\bar{K}_h$ = 0.5 and nine values of R from 0 to 0.8.	14
5.	Utilizability ϕ versus the critical ratio X for $\bar{K}_h$ = 0.4 and nine values of R from 0 to 0.8.	14
6.	Utilizability ϕ versus the critical ratio X for $\bar{K}_h$ = 0.3 and nine values of R from 0 to 0.8.	14
7.	Utilizability ϕ versus the critical ratio X for collectors with high values of concentration and five $\bar{K}_h$, from 0.3 to 0.7.	14
8.	Comparison of radiation availability for east-west and polar tracking axis at equinox, as function of cutoff time.	22
9a.	Radiation availability for concentrator with east-west axis at equinox, as function of concentration ratio C, for different values of clearness index $\bar{K}_h$.	26
9b.	Radiation availability for concentrator with polar axis at equinox, as a function of concentration ratio C, for different values of clearness index $\bar{K}_h$.	27

WORKING FIGURES

No.		Page
1.	$\bar{H}_d/\bar{H}_h$ versus $\bar{K}_h$ (Eq. II-3)	53
2.	Utilizability ϕ versus the critical ratio X for $\bar{K}_h$ = 0.7 and nine values of R from 0 to 0.8.	54
3.	Utilizability ϕ versus the critical ratio X for $\bar{K}_h$ = 0.6 and nine values of R from 0 to 0.8.	54
4.	Utilizability ϕ versus the critical ratio X for $\bar{K}_h$ = 0.5 and nine values of R from 0 to 0.8.	55
5.	Utilizability ϕ versus the critical ratio X for $\bar{K}_h$ = 0.4 and nine values of R from 0 to 0.8.	55
6.	Utilizability ϕ versus the critical ratio X for $\bar{K}_h$ = 0.3 and nine values of R from 0 to 0.8	56
7.	Utilizability ϕ versus the critical ratio X for collectors with high values of concentration and five $\bar{K}_h$, from 0.3 to 0.7.	56

LIST OF TABLES

No.		Page
I.	Function R_h and R_d for Flat Plate Collector	40
II.	Functions R_d and R_h for concentrators with fixed aperture e.g. compound parabolic concentrator (CPC)	42
III.	Functions R_h and R_d for a Collector which Tracks about East-West Axis	43
IV.	Functions R_h and R_d for collector which tracks about North-South Axis	45
V.	Functions R_h and R_d for collector with 2-axis tracking	46
VI.	Collector parameters and energy collected 15 February in New York at 50°C.	47
VII.	a) Some results of the iteration procedure to determine the cut-off time corresponding to the maximum energy (Max.$\bar{Q}_{out}$) collected.	48
VII.	b) Some results of the iteration procedure to determine the cut-off time corresponding to the maximum energy (Max.$\bar{Q}_{out}$) collected.	49
VIII.	Comparison of energy delivery for Lemont, Illinois: daily total output for central day of each month, and yearly total, in MJ per m^2 of collector aperture.	50
IX.	$\bar{H}_{coll,flat\ plate,\ tracking}$ / $\bar{H}_{coll,\ flat\ plate,\ fixed}$ ratio of radiation availability for tracking and for fixed flat plate, at equinox.	51
X.	Effect of ground reflectance, evaluated by means of the ratio of radiation availability if reflectance of ground = ρ and if brightness of ground and sky are equal.	52

THIS PAGE

WAS INTENTIONALLY

LEFT BLANK

Nomenclature

We use the symbols I for irradiance (or instantaneous insolation, in W/m^2) and H for irradiation (or daily total insolation, in J/M^2), together with subscripts b for beam (also called direct), d for diffuse and h for hemispherical (also called global or total). To minimize subscripts in the present paper we refer irradiation H (except for $\bar{H}_{coll}$) to horizontal surface, but irradiance I to normal incidence. Bars indicate long term average. Note that beam is defined with respect to the 2.8° acceptance half angle of the pyrheliometer, and not with respect to the solar disc; thus it includes the circumsolar component.[5]

A = net aperture area of collector

C = geometric (or area) concentration

F = factor to account for heat extraction or removal efficiency

H_o = extraterrestrial irradiation on horizontal surface (daily total)

$\bar{H}_{coll}$ = irradiation incident on collector aperture (daily total)

$\bar{H}_d$ = diffuse irradiation on horizontal surface (daily total)

$\bar{H}_h$ = hemispherical irradiation on horizontal surface (daily total)

I_o = solar constant = 1353 W/M^2

I_b = beam irradiance at normal incidence (pyraheliometer)

I_d = diffuse irradiance on surface normal to sun

I_h = hemispherical irradiance on surface normal to sun (pyranometer)

$\bar{K}_h = \bar{H}_h/H_o$ = long term average clearness index (called $\bar{K}_T$ in Refs. 1-4)

q_{out} = instantaneous collector output [W]

$q_\ell = AU(T_{coll} - T_{amb})$ = instantaneous collector heat loss [W]

$\bar{Q}$ = long term average energy [J] delivered by collector

$\bar{Q}_{loss}$ = long term average heat loss of collector [J]

R_d, R_h } { functions to convert horizontal irradiation to irradiation on collector aperture

$R = R_d/R_h$

t = time of day from solar noon (p.m. is positive)

t_c = collector cut off time (if $-t_{c-} = t_{c+}$)

t_{c-} = collector turn on time (hours before noon)

t_{c+} = collector turn off time (hours after noon)

t_s = sunset time

T = length of day = 24 hours = 86,400 seconds

T_a = ambient temperature

$T_f = (T_{in} + T_{out})/2$ = average fluid temperature

T_{in} = inlet fluid temperature

T_{out} = outlet fluid temperature

T_r = average receiver surface temperature

U = U-value [$W/m^2°C$)

β = collector tilt from horizontal surface (positive towards equator)

δ = solar declination

λ = geographic latitude

η_o = optical efficiency (also called $\tau\alpha$ product in the flat plate literature) = fraction of insolation absorbed by absorbed = efficiency if receiver at ambient, i.e. no heat loss.

$\bar{\eta}_o$ = long term average optical efficiency

Θ = acceptance half angle of CPC

ϕ = collector azimuth from due south, relative to horizontal plane (west is positive, east negative)

ϕ = utilizability

$\omega = 2\pi t/T$ = hour angle

$\omega = 2\pi t_s/T$ = sunset hour angle

SIMPLE PROCEDURE FOR PREDICTING LONG-TERM AVERAGE PERFORMANCE OF NONCONCENTRATING AND OF CONCENTRATING SOLAR COLLECTORS

by

Manuel Collares-Pereira* and Ari Rabl†

ABSTRACT

The Liu and Jordan method of calculating long term average energy collection of flat plate collectors is simplified (by about a factor of 4), improved, and generalized to all collectors, concentration and nonconcentrating. The only meteorological input needed are the long term average daily total hemispherical insolation $\bar{H}_h$ on a horizontal surface and, for thermal collectors the average ambient temperature. The collector is characterized by optical efficiency, heat loss (or U-value), heat extraction efficiency, concentration ratio and tracking mode. An average operating temperature is assumed. Interaction with storage can be included by combining the present model with the f-chart method of Beckman, Klein and Duffie.

A conversion factor is presented which multiplies the daily total horizontal insolation $\bar{H}_h$ to yield the long term average useful energy $\bar{Q}$ delivered by the collector. This factor depends on a large number of variables such as collector temperature, optical efficiency, tracking mode, concentration, latitude, clearness index, diffuse insolation etc., but it can be broken up into several component factors each of which depends only on two or three variables and can be presented in convenient graphical on analytical form. In general, the seasonal variability of the weather will necessitate a separate calculation for each month of the year; however, one calculation for the central day of each month will be adequate. The method is simple enough for hand calculation.

Formulas and examples are presented for five collector types: flat plate, compound parabolic concentrator, concentrator with E.-W. tracking axis, concentrator with polar tracking axis, and concentrator with two axis tracking. The examples show that even for relatively low temperature applications and cloudy climates (50°C in New York in February), concentrating collectors can outperform the flat plate.

The method has been validated against hourly weather data (with measurements of hemispherical and beam insolation), and has been found to have an average accuracy better than 3% for the long term average radiation available to solar collectors. For the heat delivery of thermal collectors the average error has been 5%. The excellent suitability of this method for

* Enrico Fermi Institute, The University of Chicago, 5630 S. Ellis Avenue, Chicago, Illinois 60637. Supported by the Instituto Nacional de Investigacão Cientifica and Centro de Fisica de Matéria Condensada, Lisbon, Portugal.

† Now on leave of absence from Argonne National Laboratory to Solar Energy Research Institute, 1536 Cole Boulevard, Golden, Colorado 80401.

comparison studies is illustrated by comparing in a location independent manner the radiation availability for several collector types or operating conditions: two axis tracking versus one axis tracking; polar tracking axis versus east-west tracking axis; fixed versus tracking flat plate; effect of ground reflectance; and acceptance for diffuse radiation as function of concentration ratio.

I. Introduction

The performance of solar collectors is usually specified in terms of instantaneous or peak efficiency, based on clear days and normal incidence. In practical applications, however, one needs to know the long term energy delivery averaged over all cloud conditions and incidence angles. To answer this need, many researchers have advocated average diurnal efficiency as a collector performance measure. Unfortunately such average efficiency curves may depend strongly on peculiarities of the weather for the test day and test location, and are therefore limited in their general applicability.

One approach to this problem is to use a computer program with instantaneous efficiency and hourly insolation data as input. The results of such a calculation can be considered valid only if the weather data are representative of long term weather behavior. Various choices have been used, for example, real hourly data for a single year, real hourly data for several years, averaged hourly data, and stochastic data. Use of real data for a specific place and year provides only a performance simulation for that place and year, but its reliability as prediction for the long term average is uncertain - after all, fluctuations in monthly total insolation from one year to the next commonly exceed ± 10%, and the resulting output fluctuations for thermal collectors are even larger.

Another drawback arises from the time, money and expertise required for computer simulations. Even though the computing time is inconsequential for a few sample simulations, the large number of parameters to be considered will make any meaningful system optimization or comparison study costly and time consuming. Furthermore one gains little intuitive understanding of functional relationships.

As an alternative we propose a generalized and simplified model of the Liu and Jordan[1] type which treats all collectors in a consistent manner and which needs as meteorological input only the long term average daily total hemispherical irradiation $\bar{H}_h$ on a horizontal surface (as well as for thermal collectors, the long term average daily ambient temperature $\bar{T}_a$). This information is readily available for a large number of locations;[1,2] Ref. 2, for example, lists 170 stations in the U.S. and Canada, and eleven stations are included in Appendix B of the present paper. The method is

simple enough for hand calculations. In general the seasonal variability of the weather will necessitate a separate calculation for each month of the year; however one calculation for the central day of each month will be adequate. Since the dependence on individual design variables such as tilt angle, concentration ratio and operating temperature is displayed explicitly, it is easy to study the effect of changing any of these variables. The influence of climate and location can be assessed systematically. This gain in intuitive understanding can be of great help for system optimization and for comparison studies. For illustration we have compared some typical collectors (flat plate, CPC, collector with east-west tracking axis, collector with polar tracking axis, and collector with 2-axis tracking).

The calculation proceeds in one or two main steps depending on the kind of solar energy system. The first step yields the long term average insolation $\overline{H}_{coll}$ reaching the collector within its acceptance angle. For collectors whose efficiency is independent or nearly independent of solar intensity nothing else is required, and the delivered energy is simply $\overline{Q} = \eta\, \overline{H}_{coll}$. This is the case for photovoltaic collectors. Thermal collectors with significant heat loss, on the other hand will be turned on only when the insolation is sufficiently high and hence the relation between $\overline{H}_{coll}$ and delivered energy $\overline{Q}$ is nonlinear. For this case the second step of the calculation is required; it depends on whether or not the average collector or storage temperature is known.

In home heating applications the average storage temperature is not known a priori, but a short hand method has been developed by S. A. Klein, et al.[2] which predicts the fraction of the load supplied by solar, taking into account the interaction with thermal storage. This method is called f-chart method and needs as input the collector parameters and the long term average insolation $\overline{H}_{coll}$ on the collector aperture (called $\overline{H}_T$ in Ref. 2). Only the collector parameters (heat removal factor, optical efficiency and U-value) and the insolation H_{coll} matter, but not the details of the collector optics. Therefore the f-chart method, which was developed only for flat plat collectors[3], can be used with any collector if $\overline{H}_T = \overline{H}_{coll}$ as calculated from our Eq. (II-I) with cutoff angle $\omega_c = \omega_s$ is inserted into

Eq. (5.4) of Ref. 2.

$$Y = A F_R' (\tau\alpha) \bar{H}_T N/L \qquad \text{(Eq. 5.4 of Ref. 2)}$$

for the abscissa of the f-chart.

For process heat and power applications f-charts have not yet been developed. However, for most applications in process heat and shaft power the collector outlet temperature is fixed or nearly fixed, and therefore one can use the utilizability method described in the classic papers of Hottel and Whillier,[4] and of Liu and Jordan.[1] We have generalized the utilizability method to all collector types. Simplification by about a factor of four relative to Ref. 1 has been achieved by defining the utilizability with respect to the day rather than the hour.[3]

The utilizability ϕ is a function of the heat loss, expressed as dimensionless critcal intensity ratio, and is defined in such a way that the delivered energy $\bar{Q}$ per aperture area A is

$$\bar{Q}/A = F \bar{\eta}_o \phi \bar{H}_{coll} \qquad \text{(I-1)}$$

where $\bar{\eta}_o$* is the average optical efficiency (which has also been called $\alpha\tau$ product); F accounts for the heat extraction or the heat removal efficiency and depends on the specification of the collector temperature (fluid inlet temperature, fluid outlet temperature, average fluid temperature or absorber surface temperature). We have recalculated ϕ for the formalism underlying out method; our ϕ curves differ markedly from those of other investigators,[1,3,4] both in interpretation and in numerical value.

Several secondary effects have not been incorporated into the present model, but could be included by straightforward modification. These effects include loss of circumsolar radiation in systems with high concentration, deviations from isotropy in the diffuse insolation, and transient losses due to collector heat capacity. The radiation correlations underlying this model equate beam radiation with radiation measured by a pyrheliometer of acceptance half angle 2.8°. For collectors with smaller acceptance angle one has to multiply $\bar{H}_{coll}$ of Eq. (II-I) by the monthly average circumsolar loss factor for the collector and location in question. Unfortunately we do not yet have enough information for a definitive answer to this question. Some preliminary analysis of circumsolar data in Ref. 5 shows that the circumsolar loss for point focus collectors will be between

*For a test procedure defining $\bar{\eta}_o$ see eq. C-17 of Appendix C.

0 and 5% for clear climates such as Albuquerque, but may reach 10% under hazy conditions (e.g., Texas in winter). Line focus collectors are less sensitive to circumsolar radiation. In the present paper we bypass this problem by assuming that any circumsolar loss factor is correctly accounted for in the measured average optical efficiency $\bar{\eta}_o$.

Under clear sky the diffuse sky radiation is not completely isotropic but somewhat centered around the sun. Consequently the 1/C rule for acceptance of diffuse radiation by a collector of concentration C tends to underestimate slightly (by about one percent) the radiation available to collectors of low concentration.[6] Long term observations of the angular distribution of sky radiation are needed before a more quantitative analysis of this effect can be made.

As for transient effects, any well designed solar collector will have warmup times much shorter than one hour, and therefore collector transients do not enter into a conventional hour-by-hour simulation. The present model also neglects collector transients. The importance of transients depends on the system and is not clear in general. Perhaps the best approach would be the development of transient loss factors which could be employed both for hourly simulation and for the present model.

In order to evaluate the accuracy of this model we have compared its predictions with the results of adding hourly contributions from weather tapes. We have avoided the usual uncertainties associated with estimating the beam component when only hemispherical insolation is known, by relying only on tapes which contain both pyranometer and pyrheliometer measurements. Such data have recently become available through the Aerospace Corporation for the five stations: Albuquerque, NM; Fort Hood, TX; Livermore, CA; Maynard, MA; and Raleigh, NC; with one to four years at each station.

We have computed the deviation

$$\varepsilon = \frac{\bar{H}_{coll,data} - \bar{H}_{coll,model}}{\bar{H}_{coll,data}} \qquad \text{(I-2)}$$

between data and model, both for a 2-axis tracker of high concentration and for a flat plate collector. (For the 2-axis tracker $\bar{H}_{coll}$ is the daily total beam radiation at normal incidence). We found that the average error

(over all stations and months) is less than 3% for the insolation $\bar{H}_{coll}$ available to the collector, both for flat plate and for concentrating collectors.[8] The model appears to be free from any significant bias with respect to location or time of year at least as far as could be discerned from this rather limited data base. For a particular month of a particular year the discrepancy between model and data can be much larger, on the order of 3% (standard deviation) for a flat plate and on the order of 10% (standard deviation) for concentrators. These fluctuations reflect the month-to-month variations in the ratio of diffuse over hemispherical insolation. Even though large, the fluctuations do not matter, provided the long term average is correct. After all, the model is designed to predict only the long term average collector performance, not the performance for a particular month.

The computation of the utilizability ϕ involves further approximations of several percent, and hence the uncertainty in the energy delivery of a thermal collector will be on the order of 5%.

In view of the evidence for the general validity of the meteorological correlations underlying the present model, we believe that the model is applicable for all locations and latitudes from -50° to +50°. We urge, however, that the model be tested again and if necessary recalibrated when long term data with pyranometer and pyrheliometer become available from a larger number of stations. The present paper provides only a users' manual.[7] The derivation of the model is documented in two companion papers, Ref. 8 for the available insolation and Ref. 9 for the calculation of the utilizability function.

II. Insolation $\bar{H}_{coll}$ Reaching Collector Aperture within Its Acceptance Angle

The long term average daily total irradiation incident on the collector within its acceptance angle is obtained from the daily hemispherical insolation $\bar{H}_h$ on a horizontal surface by means of the formula

$$\bar{H}_{coll} = [R_h - R_d \bar{H}_d/\bar{H}_h] \bar{H}_h. \qquad \text{(II-1)}$$

For the energy actually absorbed per aperture area A of the collector one has to multiply this by the average optical efficiency $\bar{\eta}_o$*

$$(\bar{Q}_{abs/A}) = \bar{\eta}_o \bar{H}_{coll} \qquad \text{(II-2)}$$

The functions R_h and R_d are given in Tables I to V, and $\bar{H}_d/\bar{H}_h$ i the long term average ratio of diffuse over hemispherical irradiation on a horizontal surface. This ratio is correlated[8] with clearness index $\bar{K}_h$ and sunset hour angle ω_s as

$$\frac{\bar{H}_d}{\bar{H}_h} = 0.775 + 0.347\ (\omega_s - \tfrac{\pi}{2}) - [0.505 + 0.261\ (\omega_s - \tfrac{\pi}{2})]\ \cos\ (2\ (\bar{K}_h - 0.9)) \qquad \text{(II-3)}$$

For nonconcentrating collectors the ω_s dependence can be neglected by setting $\omega_s = \frac{\pi}{2}$ in this equation; this curve is shown by the solid line in Fig. 1 (the dotted lines show Eq. (II-3) at $\omega_s = \frac{\pi}{2} - 0.2$ and at $\omega_s = \frac{\pi}{2} + 0.2$). The clearness index $\bar{K}_h$ is the long term average ratio

$$\bar{K}_h = \bar{H}_h/H_o \qquad \text{(II-4)}$$

of daily hemispherical insolation on a horizontal surface over H_o = extraterrestrial insolation = insolation which would have reached the same surface in the absence of any atmosphere; H_o is given by Eq. (A-1) of Appendix A.

R_h and R_d depend on collector type, collector orientation, latitude, and collector turn-on and turn-off time. We have evaluated these functions for the following collector types:

*For a test procedure defining $\bar{\eta}_o$ see appendix C - eq. C 17.

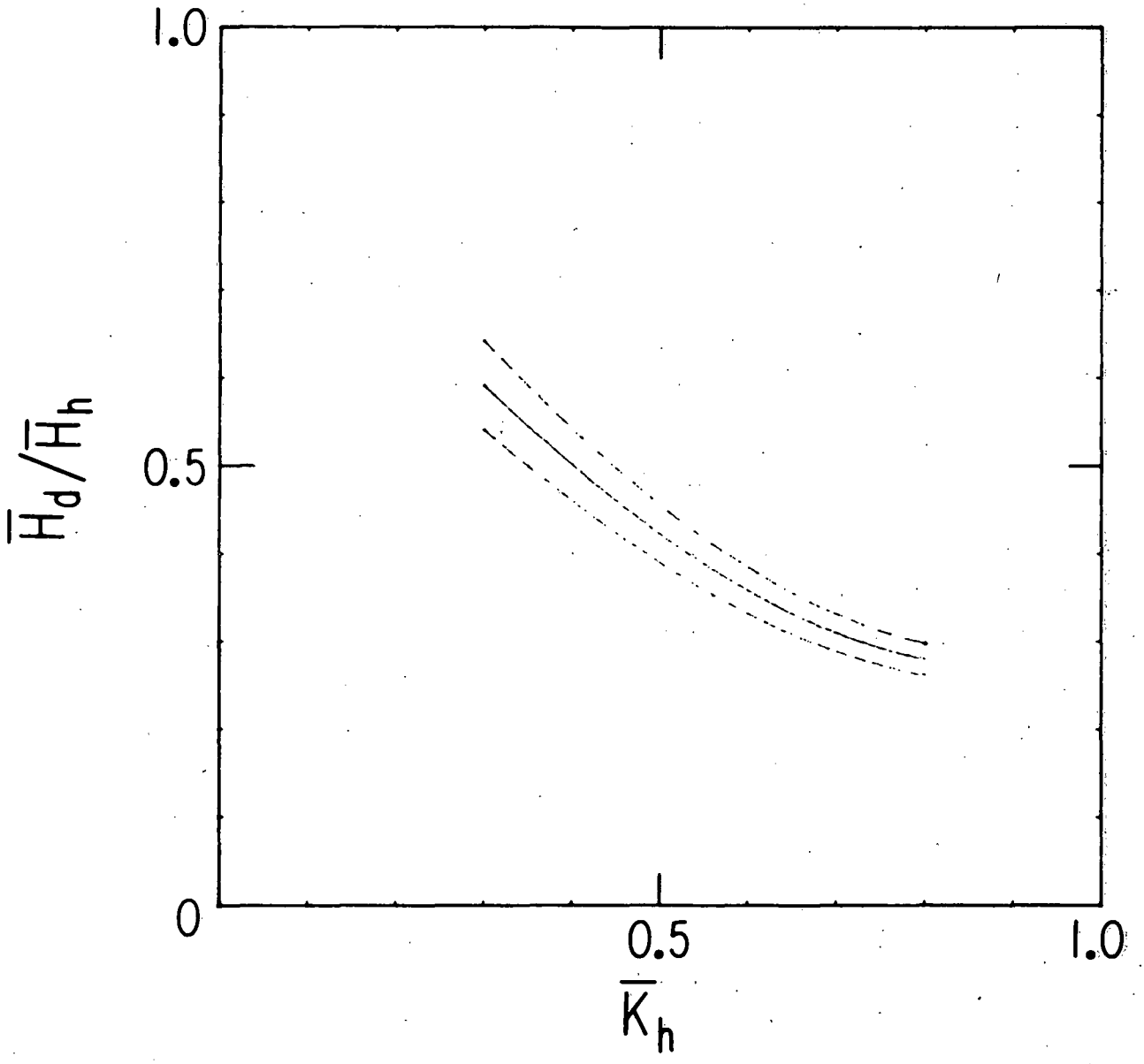

Fig. 1: $\bar{H}_d/\bar{H}_h$ versus $\bar{K}_h$ (Eq. (II-3); the solid line corresponds to $\omega_s = \pi/2$ and the dashed lines correspond to $\omega_s = \frac{\pi}{2} - 0.2$ (bottom) and $\omega_s = \frac{\pi}{2} + 0.2$ (top)

i) nonconcentrating collector with fixed aperture, e.g., flat plate collector
   a) tilt β = latitude λ, azimuth ϕ = 0 (Table 1a.)
   b) tilt $\beta \neq$ latitude λ, azimuth ϕ = 0 (Table 1b.)
   c) tilt $\beta \neq$ latitude λ, azimuth $\phi \neq 0$ (Table 1c.)

ii) Concentrators with fixed aperture, azimuth ϕ = 0
   e.g., compound parabolic concentrator (= CPC)
   a) tilt β = latitude λ (Table IIa.)
   b) tilt $\beta \neq$ latitude λ (Table IIb.)

iii) One-axis tracker of concentration C, tracking about east-west horizontal axis (Table III)

iv) One-axis tracker of concentration C, tracking about north-south axis of tilt β
   a) tilt β = latitude λ (= polar mount) (Table IVa.)
   b) tilt $\beta \neq$ latitude λ (Table IVb.)

v) Two-axis tracker of concentration C (Table V.)

Table II applies also to high concentration systems with fixed reflector and tracking receiver such as the hemispherical reflector[12] and the segmented cylindrical reflector[13] (developed by General Atomic), provided their internal shading effects are included in the long term average optical efficiency $\bar{\eta}_o$.

Tables III to IV hold for both reflective (mirror) and refractive (lens) concentrators if the aperture moves as a single unit; included is almost any reasonable solar concentrator with trough or dish reflector or with Fresnel lens. This is in contrast to Fresnel reflector systems, e.g., the power tower,[12] whose aperture consists of reflector segments which follow the sun individually; for this latter case use of Tables III to V is not quite correct. If more accurate formulas are needed for Fresnel reflectors, they can be derived by the method described in Ref. 9. For linear Fresnel reflectors with east-west axis linear interpolation between the results obtained from Tables II and III should be adequate.

We find it convenient to express all times t in dimensionless form as hour angle ω from solar noon

$$\omega = \frac{2\pi t}{T} \quad \text{with T = length of day = 24 hr;} \qquad \text{(II-5)}$$

note that throughout this paper all angles are in radians, except for a few cases where degrees are explicitly indicated. The sunset hour angle

$$\omega_s = \frac{2\pi t_s}{T}$$

corresponding to sunset hour t_s is given by

$$\cos \omega_s = -\tan \lambda \tan \delta \qquad \text{(II-6)}$$

where λ = geographic latitude
and δ = solar declination given by Eq. (A-2) of Appendix A. The quantities a, b and d in these tables are functions of ω_s

$$a = 0.409 + 0.5016 \sin (\omega_s - 1.047) \qquad \text{(II-7a)}$$

$$b = 0.6609 - 0.4767 \sin (\omega_s - 1.047) \qquad \text{(II-7b)}$$

and

$$d = \sin \omega_s - \omega_s \cos \omega_s \qquad \text{(II-7c)}$$

(Note that 1.047 radians = 60°). In the equations for flat plate and CPC ω_s' is the sunset hour angle on the collector aperture tilted at an angle β from the horizontal and given by

$$\cos \omega_s' = -\tan (\lambda - \beta) \tan \delta. \qquad \text{(II-8)}$$

The reflectance ρ of the ground in front of a flat plate collector is also needed for Table I; recommended[12] values are $\rho = 0.7$ with, and $\rho = 0.2$ without snow, in the absence of better information.

One further variable remains to be explained, the collector cut-off time t_c, or equivalently, the cut-off angle

$$\omega_c = \frac{2\pi t_c}{T} \qquad \text{(II-9)}$$

If the collector is placed due south, i.e. with zero azimuth, and if its time constant is short, it will operate symmetrically around solar noon, being turned on at

$$\text{turn-on time } t_{c-} = -t_c \tag{II-10a}$$

and turned off at

$$\text{turn-off time } t_{c+} = t_c \ . \tag{II-10b}$$

This has been assumed for all collectors with zero azimuth. For the flat plate with nonzero azimuth the asymmetric turn-on and turn-off angles are explicitly shown, with the sign convention that ω_{c-} (morning) is negative and ω_{c+} (afternoon) is positive, as in Eq. (II-10). If collectors with zero azimuth are operated with $\omega_{c-} \neq -\omega_{c+}$ to account for transient effects or for asymmetric shading problems, the formulas of Table I to V can still be used in the combination

$$R_{\text{effective}} = \frac{1}{2} [R(-\omega_{c-}) + R(\omega_{c+})]. \tag{II-11a}$$

When $-\omega_{c-}$ and ω_{c+} do not differ very much, the simple approximation

$$R_{\text{effective}} \approx R\left(\omega_c = \frac{-\omega_{c-} + \omega_{c+}}{2}\right) \tag{II-11b}$$

is acceptable.

The model has been written for explicit input of cut-off time t_c in order to permit greater flexibility and applicability in situations with any shading configuration. The cut-off time is limited by optical constraints, and may be further reduced by thermal considerations for thermal collectors. The procedure of finding t_c for thermal collectors is described in Section III.

The highest possible value of ω_c is the sunset hour angle ω_s for a completely unshaded collector. For fixed collectors ω_c also has to be less than ω_s of Eq. (II-8) except in the unlikely case of a collector which can operate on diffuse radiation alone. In collector arrays some shading between adjacent rows will usually occur close to sunrise and sunset, and ω_c has to be calculated from the trigonometry of the collector array. This is straightforward for an array with continuous collector rows, for example with long horizontal parabolic troughs. For arrays with rows of separate collector units, for example parabolic dishes, the analysis of shading is more complicated. In either case a good albeit slightly optimistic approximation is obtained by setting t_c

equal to the time at which half of the collector aperture is shaded.

For nontracking concentrators of the CPC type[15-17] the optical cutoff time depends on the acceptance half angle θ of the collector. If a trough-like CPC with east-west axis is mounted at tilt β = latitude λ, ω_c is given by

$$\cos \omega_c = \frac{\tan |\delta|}{\tan \theta} \qquad \text{(II-12)}$$

For CPCs with concentration $C > 2$ the tilt will generally differ from the latitude, with tilt adjustments during the year, and ω_c is given by

$$\cos \omega_c = \frac{\tan \delta}{\tan (\lambda - \beta + \theta \, \delta/|\delta|)} \qquad \text{(II-13)}$$

Note that for a CPC with tilt adjustments one should always verify that the sun at noon is within the acceptance angle.

III. Heat Loss, Utilizability, and Cutoff Time

If all days and hours were identical, $\bar{Q}$ could be obtained by simply subtracting the total daily heat loss

$$(\bar{Q}_{loss}/A) = 2 \, t_c \, U(\bar{T}_{coll} - \bar{T}_{amb}) \qquad \text{(III-1a)}$$

from the absorbed solar energy $\bar{\tau}_o \bar{H}_{coll}$; $\bar{T}_{coll}$ is the operating temperature of the collector (absorber surface or fluid temperature, depending on choice of temperature base in Appendix C). Since the heat loss from transport lines between collector and storage or point of use occurs at the same time as the loss from the collector, i.e. only when the circulating pump is turned on, the equation for $\bar{Q}_{loss}$ should really include the loss q_{line} from the transport lines (which depends of course on the installation)

$$\bar{Q}_{loss} = 2t_c [AU \, (\bar{T}_{coll} - \bar{T}_{amb}) + q_{line}] \, . \qquad \text{(III-1b)}$$

Due to the variability of the weather, the true energy gain can be significantly higher. This feature can be illustrated by the following two artificial climates. Climate 1 has identical days, all uniformly overcast, while climate 2 has clear days half of the time and no sunshine for the rest; both climates have the same long term average insolation $\bar{H}$. If the heat loss of a collector equals the peak insolation of climate 1, no useful energy can be collected. Under climate 2, however, the same collector can collect some useful energy on the clear days.

It is convenient to calculate this affect once and for all for any concentrator type and for any climate, and to summarize the result in terms of the utilizability function ϕ • ϕ depends on the critical intensity ratio

$$X = \frac{(\bar{Q}_{loss}/A)}{\bar{\eta}_o \bar{H}_{coll}} \qquad \text{(III-2)}$$

and is defined in such a way that the long term average collected energy $\bar{Q}$ per aperture area A is

$$\bar{Q}/A = F\ \phi\ \bar{\eta}_o\ \bar{H}_{coll} \qquad \text{(I-1)}$$

where F is the heat extraction or heat removal efficiency factor. F depends on the type of operating temperature which has been specified, as discussed in Appendix C, and is given by

$$F = \begin{cases} 1 \text{ for average receiver surface temperature } T_r \\ F' \text{ of Eq. (C-5) for average fluid temperature } T_f \\ F_R \text{ of Eq. (C-7) for fluid inlet temperature } T_{in} \\ F_R/[1-F_R UA/(\dot{m}C_p)] \text{ of Eq. (C-8) for fluid outlet temperature } T_{out} \end{cases} \qquad \text{(III-3)}$$

The calculation up to and including ϕ is the same regardless of which temperature base (T_{in}, T_{out}, T_f or T_r) is used to specify the instantaneous efficiency. Only at the last step the temperature base is accounted for by inserting the appropriate factor F in Eq. (I-1) for $\bar{Q}$.

In principle, ϕ is a complicated function of many variables, but fortunately the dependence on most of these is rather weak. For the climatic variation, Liu and Jordan[1] have shown that consideration of a single factor, the clearness index $\bar{K}_h$ (see Eq. II-4) is adequate. From a large number of numerical simulations[9], we conclude that ϕ can be approximated within a few percent by a function of only three variables, the clearness index $\bar{K}_h$, the ratio

$$R = \frac{R_d}{R_h} \qquad \text{(III-4)}$$

and the critical intensity ratio X of Eq. (III-2).

For nontracking collectors, ϕ is given by the parametric expressions

$$\phi = \exp\,[-X+(0.337 - 1.76\,\bar{K}_h + 0.55R\,)X^2] \qquad \text{(III-5a)}$$

for $0.3 \lesssim \bar{K}_h \lesssim 0.5$ and $0 \lesssim X \lesssim 1.2$,

and

$$\phi = 1-X + (0.50 - 0.67\,\bar{K}_h + 0.25R)\,X^2 \qquad \text{(III-5b)}$$

for $0.5 \lesssim \bar{K}_h \lesssim 0.75$ and $0 \lesssim X \lesssim 1.2$

For tracking collectors of high concentration ($C \gtrsim 10$), the R dependence can be neglected and the fit

$$\phi = 1- (0.049 + 1.44\,\bar{K}_h)\,X + 0.341\,\bar{K}_h\,X^2 \qquad \text{(III-5c)}$$

can be used for all values of $\bar{K}_h \lesssim 0.75$ and for $0 \lesssim X \lesssim 1.2$. For exceptionally clear climates, i.e., with $\bar{K}_h \gtrsim 0.75$, the simple expression

$$\phi = 1 - X \text{ for } \bar{K}_h \gtrsim 0.75 \qquad \text{(III-5d)}$$

should be used for all collector types. These ϕ curves are shown in Figs. 2 to 7.

The fits were derived with emphasis on accuracy at reasonably large values of ϕ because collectors with low utilizability will not collect enough energy to be economical. The above expressions for ϕ are reliable whenever ϕ is larger than approximately 0.4. At smaller values of ϕ, the above

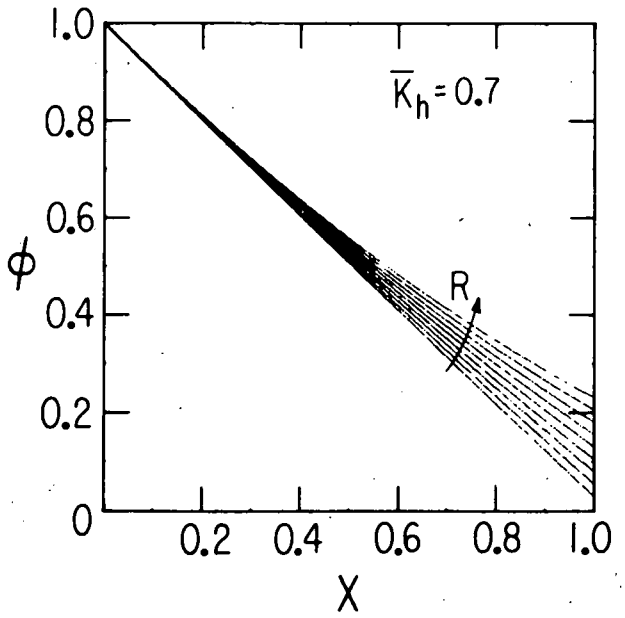

Fig. 2: Utilizability ϕ versus the critical ratio X for $\bar{K}_h$ = 0.7 and nine values of R from 0 to 0.8.

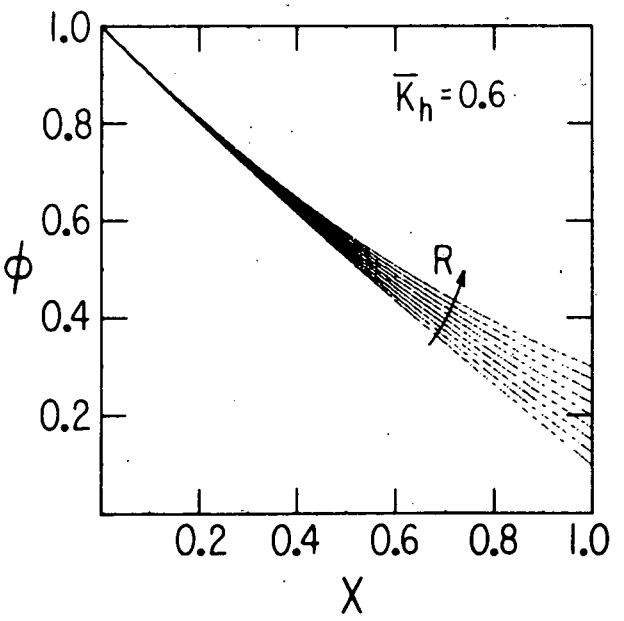

Fig. 3: Utilizability ϕ versus the critical ratio X for $\bar{K}_h$ = 0.6 and nine values of R from 0 to 0.8.

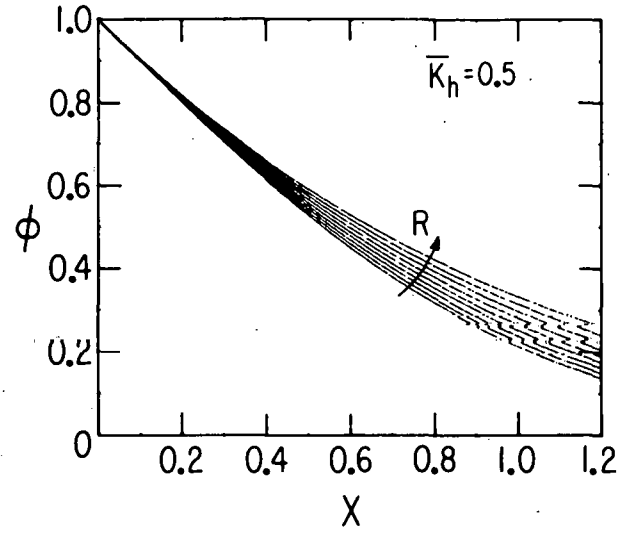

Fig. 4: Utilizability ϕ versus the critical ratio X for $\bar{K}_h$=0.5 and nine values of R from 0 to 0.8.

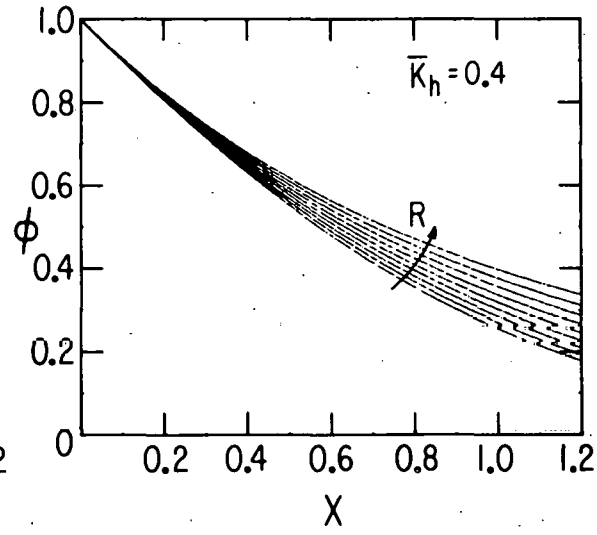

Fig. 5: Utilizability ϕ versus the critical ratio X for $\bar{K}_h$=0.4 and nine values of R from 0 to 0.8.

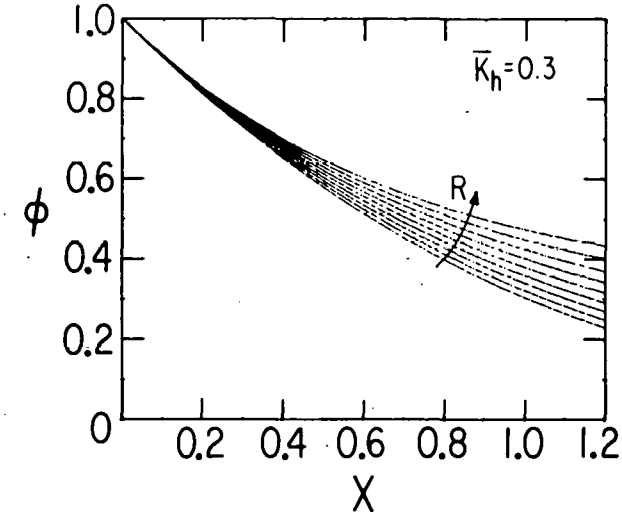

Fig. 6: Utilizability ϕ versus the critical ratio X for $\bar{K}_h$=0.3 and nine values of R from 0 to 0.8.

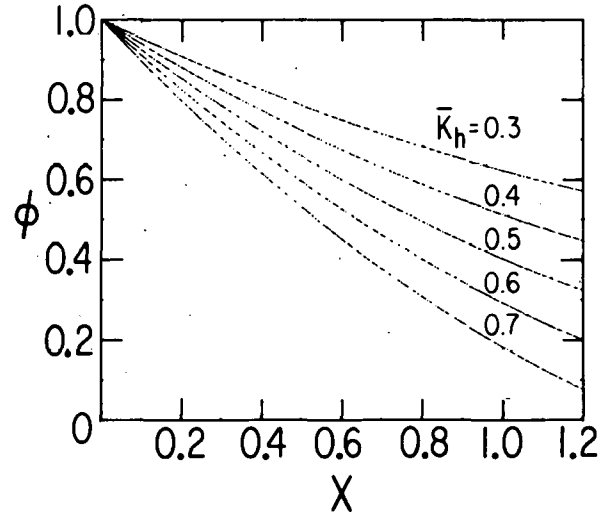

Fig. 7: Utilizability ϕ versus the critical ratio X for collectors with high values of concentration and five $\bar{K}_h$, from 0.3 to 0.7.

fits are not recommended (nor is it likely that a collector will be practical if its heat loss is so large as to imply $\phi \lesssim 0.4$). Since the above fits may increase with X at very large X, they must not be used outside the specified range of X-values.*

The values of R will range from about -0.1 to 0.8 for nontracking collectors and from 0.95 to 1.05 for collectors with high concentration. For tracking collectors with significant acceptance for diffuse radiation (i.e., ($C \lesssim 10$), R may fall between 0.8 and 1.0. For such a configuration, we recommend linear interpolation in R between the R = 0.8 value of Eqs. (III-5a) or (5b) and Eq. (III-5c) assuming that the latter equation corresponds to R = 1.0. (This is not very accurate because the variation of with R in this range is not uniform for all $\bar{K}_h$; but in any case, tracking thermal collectors of very low concentration appear to have little practical interest.)

The cutoff time t_c for thermal collectors can be determined by the following simple iteration procedure (which is justified in Ref. 9):

i) start with $t_c = t_{c1}$ = maximum permitted by optics, as discussed at the end of the previous section; for example, $t_{c1} = t_s$ for flat plate or for tracking collectors if there is no shading. For the CPC, t_{c1} is given by Eqs. (II-12) or (II-13).

ii) calculate corresponding output $\bar{Q}_1$.

iii) decrease t_c by Δt_c to get new $t_{c2} = t_{c1} - \Delta t_c$ (Δt_c = 0.5 hr will give sufficient accuracy in most cases).

iv) calculate output $\bar{Q}_2$ for t_{c2} and repeat procedure until maximal $\bar{Q}$ is found.

The smaller the heat loss, the closer the optimal t_c will be to t_{c1}. This is illustrated by the sample calculations in Tables VI and VII which were carried out with a rather small decrement Δt_c = 0.1 hour. This small value was chosen only for the sake of illustration. For example in Table VIIa a value of Δt_c = 0.5 hr would have yielded $\bar{Q}$ = 3.714 MJ/m^2 on the second interation, 1% less than the value of 3.743 MJ/m^2 obtained with

*One could extend the utilizability curves beyond x = 1.2 by drawing tangents at x = 1.2. However, for reasons explained in Ref. 9, accuracy cannot be guaranteed.

Δt_c = 0.1 hr on the 14th iteration.
The maximum is broad and quite insensitive to uncertainties in t_c.

IV. Sample Calculation

To provide an example, we calculate the energy delivery of several collector types in New York, N.Y., on February 15. The latitude is $\lambda = 40.5°$ and the sunset time $t_s = 5.24$ hr. The relevant values of insolation $\bar{H}_h$, clearness index $\bar{K}_h$ and daytime ambient temperature $\bar{T}_a$ are given in Appendix B as

$$\bar{H}_h = 8.33 \times 10^6 \text{ J/m}^2 \text{ per day}$$

$$\bar{K}_h = 0.41$$

$$\bar{T}_a = 1.0°\text{C}$$

The correlation for the diffuse/hemispherical ratio

$$\frac{\bar{H}_d}{\bar{H}_h} = 0.775 + 0.347 \left(\omega_s - \frac{\pi}{2}\right) - [0.505 + 0.261 \left(\omega_s - \frac{\pi}{2}\right)] \cos\left(2 \left(\bar{K}_h - 0.9\right)\right) \qquad \text{(II-3)}$$

yields a diffuse component of $\bar{H}_d = 3.78 \times 10^6$ J/m^2 per day for these conditions. For the ground reflectance we assume $\rho = 0.2$.
We consider the following five collectors:

i) Flat plate collector with optical efficiency $\bar{\eta}_o = 0.75$, U-value U = 4.0 W/m^2 C, and heat extraction efficiency factor F' = 0.90, typical of double glazing and selective coating.

ii) Fixed CPC collector with evacuated receiver, having $\bar{\eta}_o = 0.60$, U = 0.8 W/m^2 C, F' = 0.99, concentration C = 1.5 and acceptance angle 2 θ = 68°. These values are typical of the present generation of CPC collectors, for example the 1.5 X CPC described in Ref. 18. The heat extraction efficiency F' is excellent because of the combination of vacuum and selective coatings in the receiver (even if air is used as heat transfer fluid).

iii) One-axis tracking concentrator with east-west axis (horizontal) and collector parameters $\bar{\eta}_o = 0.65$, U = 0.7 W/m^2 C, F' = 0.95 and C = 20. These values are typical of good collectors with parabolic trough reflectors and single glazed nonevacuated selective receivers.[19]

iv) Same collector as iii) but with polar mount, i.e. tracking axis in north-south direction with tilt equal latitude.

v) Two axis tracker of high concentration, for which we arbitrarily assume $\bar{\eta}_o = 0.65$, $U = 0.2 W/m^2$ C, $C \approx 500$ and $F' = 0.9$ because no reliable test data are available for such a collector at the present time.

The above collector parameters represent currently available technology. All collectors stand to gain from improvements in reflector materials, low cost antireflection coatings and selective surfaces. The magnitude of the gains to be expected varies from collector to collector. Of the collectors we have considered, the evacuated CPC has the lowest optical efficiency, because of double glazing, losses in the reflector, and low absorptivity of currently available selective coatings on glass;[14,20] it therefore offers the greatest potential for improvement. Optical efficiencies above 0.70 have recently been demonstrated for evacuated CPC collectors.[18] The collector parameters are listed in the first four rows of Table VI.

For the operating temperature we consider two possibilites, either average receiver surface temperature $\bar{T} = 50°C$ or average fluid temperature $\bar{T}_f = 50°$; this temperature is in the range appropriate for space heating applications. The calculation up to and including ϕ is the same regardless of which temperature base (T_{in}, T_{out}, T_f or T_r, see Appendix C) is used to specify the instantaneous efficiency. Only at the last step the temperature base is accounted for by inserting the corresponding factor F in the equation

$$\bar{Q} = AF\bar{\eta}_o \phi \bar{H}_{coll} \qquad (I-1)$$

As discussed in Section II, the values for F are

1 for average receiver surface temperature T_r

F' of Eq. (C-5) for average fluid temperature T_f

F_R of Eq. (C-7) for fluid inlet temperature T_{in}

$F_R/[1-F_R UA/(\dot{m}C_p)]$ of Eq. (C-8) for fluid outlet temperature T_{out}

The entries in Table VI are obtained by iteration over t_c with $\Delta t_c = 0.1$ hr; details of the intermediate iterations are provided in Table VII. Rows 5

We have neglected line losses in this comparison because in such an application line losses would be nearly the same for all collector types.

to 8 list the cutoff time t_c, the functions R_h and R_d of Tables I to V, and the ratio $R = R_d/R_h$. The insolation $\bar{H}_{coll}$ incident on the aperture during operating hours is obtained from Eq. (II-1) $\bar{H}_{coll} = [R_h - R_d \bar{H}_d/\bar{H}_h] \bar{H}_h$ and listed in Row 9. $\bar{H}_{coll}$ reflects several competing influences: on one hand the gain of diffuse radiation for the flat plate, and on the other hand the longer collection time due to reduced heat losses for concentrating collectors.

Row 10 lists the critical intensity ratio $X = \bar{Q}_{loss}/(A\, \bar{\eta}_o \bar{H}_{coll})$ of Eq. (III-2), and the corresponding value of the utilizability ϕ of Eq. (III-5) is entered in Row 11. The final result for the delivered energy $\bar{Q}/A$ at specified receiver surface temperature $T_r = 50°C$ is given in Row 12. If a different temperature base was specified, the result in Row 12 is simply multiplied by the appropriate factor for heat extraction or removal efficiency. Row 13 gives the energy delivered $\bar{Q}/A$ if the average fluid temperature is $T_f = 50°C$; it is the product of $\bar{Q}/A$ of Row 12 and the heat extraction efficiency F' in Row 4.

The large cutoff time t_c for the tracking collectors results from the assumed absence of any shading. In practical installations t_c is likely to be reduced by about 1/2 hr to 1 hr, and the energy output will be on the order of ten percent lower. However, even with severe shading and 20% reduction of $\bar{Q}$ the tracking collectors would still be as good as (for east-west axis) or much better than the flat plate. The cutoff times for the CPC and the flat plate are realistic and unaffected by shading in any reasonable installation. The good performance of the CPC compared to the parabolic trough with east-west tracking axis is due to its ability to collect most of the diffuse insolation. Collectors with polar tracking axis or with two-axis tracking can deliver significantly more heat per aperture area than fixed collectors or collectors with east-west axis. On the other hand, considerations of field layout, plumbing connections and line losses may make concentrators with east-west axis more attractive for large installations.

To evaluate the effect of different operating temperatures on long term average performance, we list in Table VIII the energy output of the above mentioned collectors for operation at several temperatures, including

ambient. The location is Lemont, Illinois, a suburb of Chicago.[21]

The examples show that even in relatively cloudy climates and even for rather low temperatures (e.g. space heating) concentrating collectors can significantly outperform the flat plate. This conclusion stands in strong contrast to the conventional wisdom that concentrating collectors are impractical for such applications. It is consistent with findings of recent studies[22,23] of insolation availability (i.e., $\bar{H}_{coll}$) for various collector types and climatic regions. It is important to underscore the performance potential of concentrating collectors at a time when such collectors are beginning to enter the market at cost nearly competitive with flat plate collectors.[24] Since the concentrator industry is still undeveloped compared to the flat plate industry, and since the materials requirements can be smaller, much greater cost reductions can be expected than for flat plates. Therefore, the conventional wisdom is likely to be wrong, and concentrating collectors may replace flat plates for many applications.

V. Comparison Studies

In this section we demonstrate the use of our method for comparison studies by evaluating and comparing in a location independent manner the energy availability for various collector types and operating conditions: A. two axis tracking versus one axis tracking; B. polar tracking axis versus east-west tracking axis; C. fixed versus tracking flat plate; D. effect of ground reflectance; and E. acceptance for diffuse radiation as a function of concentration ratio. For cases B through D we consider only equinox since this section is to be just an illustration, not an exhaustive study. At equinox $\omega_s = \frac{\pi}{2}$, the declination vanishes, and the coefficients a, b and d of Tables I to V are

$$a = 0.6598 \qquad b = 0.4226 \qquad d = 1.0 \tag{V-1}$$

while the ratio (II-3) of diffuse over hemispherical insolation becomes

$$\left.\frac{\bar{H}_d}{\bar{H}_h}\right|_{\omega_s = \frac{\pi}{2}} = 0.775 - 0.505 \cos\left(2(\bar{K}_h - 0.9)\right) \tag{V-2}$$

A. One Axis (Polar) Tracking versus Two Axis Tracking

By tracking with two degrees of freedom one keeps the collector normal to the sun at all times and has more radiation available than with one axis tracking. As for total radiation available during the day the difference between a polar mounted one axis tracker and a two axis tracker can easily be evaluated from the equations for R_d and R_h in Tables IV and V. For simplicity we assume high concentration to neglect the 1/C contribution of diffuse radiation. Since both R_d and R_h differ only by a factor cos δ between these collectors, the available radiation differs also by this factor:

$$\frac{H_{\text{coll, 1 axis polar}}}{\bar{H}_{\text{coll, 2 axis}}} = \cos \delta \qquad \text{(V-3)}$$

where δ is the solar declination. The cosine of the declination varies only from 0.9 to 1.0 during the year, and therefore the difference is rather small, even at solstice. In practice this difference may be enhanced (perhaps doubled) by end effects if the polar axis tracker has no end reflectors; this depends of course on the optical design.

B. Polar versus East-West Tracking Axis

In the following subsections we consider only equinox; then the sun moves in a plane and the formulas for nontracking (Table II) and for tracking (Table III) concentrators with east-west axis become identical. For high concentrations the functions R_d and R_h become in this case

$$R_d \left(\omega_s = \frac{\pi}{2}\right)\Big|_{\text{EW axis}} = \frac{\sin \omega_c}{\cos \lambda} \qquad \text{(V-4)}$$

and

$$R_h \left(\omega_s = \frac{\pi}{2}\right)\Big|_{\text{EW axis}} = \frac{1}{\cos \lambda} \{0.6598 \sin \omega_c + 0.2113(\cos \omega_c \sin \omega_c + \omega_c)\} \qquad \text{(V-5)}$$

The irradiation available to a concentrator with east-west tracking axis is therefore

$$\bar{H}_{coll,\ EW} = [0.6598 \sin \omega_c + 0.2113 (\cos \omega_c \sin \omega_c + \omega_c) - \frac{\bar{H}_d}{H_h} \sin \omega_c] \frac{\bar{H}_h}{\cos \lambda} , \qquad (V-6)$$

with $\bar{H}_d/\bar{H}_h$ given by Eq. (III-2). For a concentrator with polar tracking axis the available irradiation is

$$\bar{H}_{coll,\ polar} = [0.6598\ \omega_c + 0.4226 \sin \omega_c - \frac{\bar{H}_d}{\bar{H}_h} \omega_c] \frac{\bar{H}_h}{\cos \lambda} \qquad (V-7)$$

which is the same as for the two-axis tracker, the time of year being equinox. To compare the collectors and display the dependence on cutoff angle ω_c we have plotted in Fig. 8 the ratio (lower curves)

$$\frac{\bar{H}_{coll,EW}\ (\omega_s = \frac{\pi}{2}\ ,\ \omega_c)}{\bar{H}_{coll,polar}\ (\omega_s = \frac{\pi}{2}, \omega_c = \frac{\pi}{2})}$$

and the ratio (upper curves)

$$\frac{\bar{H}_{coll,\ polar}\ (\omega_s = \frac{\pi}{2}\ ,\ \omega_c)}{\bar{H}_{coll,\ polar}\ (\omega_s = \frac{\pi}{2}\ ,\ \omega_c = \frac{\pi}{2})}$$

versus ω_c. The sensitivity of these quantities to the diffuse/hemispherical ratio is relatively small, as shown by the fact that the curves for $\bar{K}_h = 0.4$ are close to those for $\bar{K}_h = 0.7$. These ratios are independent of geographic latitude.

Clearly, the polar tracking axis exceeds the east-west tracking axis in potential for energy collection. But, despite a difference of 20 to 30% (and even more for thermal collectors) one will usually choose a horizontal tracking axis for large concentrator arrays in order to minimize expenses and heat losses due to heat transfer lines. On the other hand, in small installations with a single row of concentrator modules, the polar axis mount is likely to be preferred. In a home heating or cooling system, for example, lightweight polar mounted reflector troughs could be

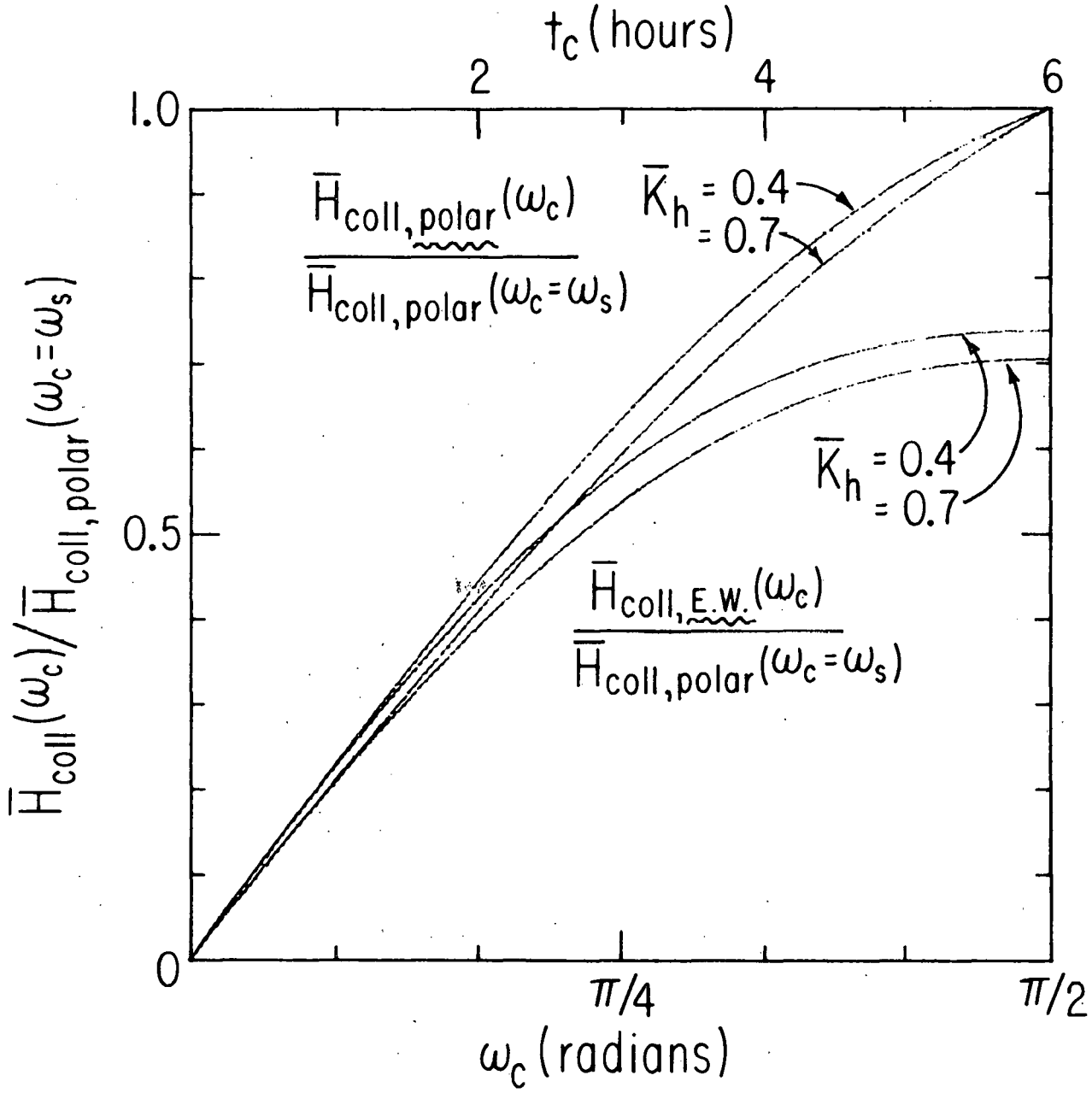

Fig. 8. Comparison of radiation availability for east-west and polar tracking axis at equinox, as function of cutoff time.

placed under a glass roof, an arrangement which minimizes problems with windloading and dirt on the reflector.

C. Flat Plate: Fixed versus Tracking

The enhanced radiation availability for tracking surfaces has led some investigators to consider the possibility of tracking a flat plate collector. We do not wish to take sides in a debate whether such an arrangement could ever be practical, and present this paragraph only for the sake of illustration.

Strictly speaking Tables III to V with C = 1 do not quite correspond to a tracking flat plate because of differences in brightness of ground and of sky. However, as shown in the following subsection, neglect of this difference results only in errors of the order of 1 to 4%, for collectors with tilt less than 40°. Furthermore, a comparison between fixed and tracking flat plates is hardly effected at all by this difference, if both are based on formulas which consistently equate the brightness of ground and of sky. Working at equinox we can represent a fixed flat plate with tilt = latitude by Table III and a two axis tracking (or a polar axis tracking) flat plate by Table V, provided the concentration ratio C is set equal to 1.0. The resulting radiation availabilities are

$$\bar{H}_{\text{coll, flat plate, fixed}} \left(\omega_s = \frac{\pi}{2}\right) = \left[0.6598 \sin \omega_c + 0.2113 \left(\cos \omega_c \sin \omega_c + \omega_c\right) - \sin \omega_c \left(1 - \cos \lambda\right) \frac{\bar{H}_d}{\bar{H}_h}\right] \frac{\bar{H}_h}{\cos \lambda} \qquad \text{(V-8)}$$

and

$$\bar{H}_{\text{coll, flat plate , tracking}} \left(\omega_s = \frac{\pi}{2}\right) = \left[0.6598\, \omega_c + 0.4226 \sin \omega_c - \left(\omega_c - \sin \omega_c \cos \lambda\right) \frac{\bar{H}_d}{\bar{H}_h}\right] \frac{\bar{H}_h}{\cos \lambda} \qquad \text{(V-9)}$$

The ratio of these two quantities is listed in Table IX for different values of latitude and clearness index. The enhancement in available radiation increases with latitude and clearness index, from about 13% to 33%.

D. Effect of Ground Reflectance

In the preceding subsection we compared radiation availability to fixed and to tracking flat plate collectors by neglecting the difference in brightness between ground and sky. The effect of the ground reflectance on flat plate collector performance can readily be evaluated by means of Table I. For equinox and tilt = latitude Table I yields

$$R_{d\ \text{flat plate}}\ (\omega_s = \tfrac{\pi}{2}) = [\frac{1}{\cos\lambda} - \frac{1}{2}(1 + \cos\lambda)] \sin\omega_c \qquad \text{(V-10)}$$

and

$$R_{h\ \text{flat plate}}\ (\omega_s = \tfrac{\pi}{2}) = [\frac{1}{\cos\lambda} + \frac{\rho}{2}(1 - \cos\lambda)]$$

$$\times\ [0.6598 \sin\omega_c + 0.2113\ (\cos\omega_c \sin\omega_c + \omega_c)] \qquad \text{(V-11)}$$

where ρ is the reflectance of the ground in front of the collector. If the brightness of ground and sky were equal, the $\frac{1}{2}(1 + \cos\lambda)$ term in Eq. (V-10) could be replaced by one and the $(1 - \cos\lambda)$ term in Eq. (V-11) replaced by zero; the resulting $\bar{H}_{coll}$ would be just Eq. (V-8).

To evaluate the effect of the ground reflectance ρ we list in Table X the ratio

$$\frac{\bar{H}_{coll,\ \text{flat plate, ground = sky}}\ (\omega_s = \frac{\pi}{2},\ \omega_c = \frac{\pi}{2})}{\bar{H}_{coll,\ \text{flat plate, ground =}\ \rho}\ (\omega_s = \frac{\pi}{2},\ \omega_c = \frac{\pi}{2})}$$

for different values of latitude and clearness index. For latitudes beyond 30° the sensitivity to ρ increases, and we have included the $\rho = 0.7$ case (for snow) in addition to $\rho = 0.2$. The ratio of radiation available with and without snow can readily be obtained from Table X. For example, for latitude 40° and clearness index 0.5 this ratio is

$$\frac{\bar{H}_{coll,\ \text{flat plate},\ \rho = 0.7}}{\bar{H}_{coll,\ \text{flat plate},\ \rho = 0.2}} = \frac{1.02}{0.97} = 1.05$$

One learns from this table that the error due to neglect of difference between sky and ground reflectance is negligible for tilt below 20° and small (1 to 4%) even for tilt of 40°.

E. Collection of Diffuse Radiation as Function of Concentration

The R_d and R_h functions for concentrators of low concentration C contain a term proportional to 1/C to account for their ability to accept part of the diffuse radiation. By decreasing C, one can collect more of the diffuse component, but at the price of increasing the receiver surface and the heat losses. A complete optimization of the concentration ratio should take into account several additional factors, in particular mirror and tracking errors and circumsolar radiation - an undertaking beyond the scope of the present paper. But, to provide at least some evaluation of the importance of the diffuse component, we have calculated the insolation available to a concentrator with east-west axis at equinox (from Table II or III) as a function of concentration C

$$\bar{H}_{coll,\ EW,\ conc} = C^{(\omega_s = \frac{\pi}{2})} = [0.6598 \sin \omega_c + 0.2113 (\sin \omega_c \cos \omega_c + \omega_c) - \frac{\bar{H}_d}{\bar{H}_h} (1 - \frac{\cos \lambda}{C}) \sin \omega_c] \frac{\bar{H}_h}{\cos \lambda} \qquad (V\text{-}12)$$

Fig. 9a shows the ratio

$$\frac{\bar{H}_{coll,\ EW,\ Conc=C\ (\omega_s = \frac{\pi}{2},\ \omega_c = \frac{\pi}{2})}}{\bar{H}_{coll,\ EW,\ Conc\ =\ 1^{(\omega_s = \frac{\pi}{2},\ \omega_c = \frac{\pi}{2})}}} = \frac{.9917 - \frac{\bar{H}_d}{\bar{H}_h} [1 - \frac{\cos \lambda}{C}]}{.9917 - \frac{\bar{H}_d}{\bar{H}_h} [1 - \cos \lambda]} \qquad (v\text{-}13)$$

for different values of the clearness index and latitude λ=35°.
The analogous ratio for concentrators with polar tracking axis is

$$\frac{\bar{H}_{coll,\ polar,\ conc=C^{(\omega_s = \frac{\pi}{2},\ \omega_c = \frac{\pi}{2})}}}{\bar{H}_{coll,\ polar\ conc\ =\ 1^{(\omega_s = \frac{\pi}{2},\ \omega_c = \frac{\pi}{2})}}} = \frac{1.459 - \frac{\bar{H}_d}{\bar{H}_h} \cdot (\frac{\pi}{2} - \frac{\cos \lambda}{C})}{1.459 - \frac{\bar{H}_d}{\bar{H}_h} \cdot (\frac{\pi}{2} - \cos \lambda)} \qquad (V\text{-}14)$$

This is shown in Fig. 9b also evaluated at λ = 35°. The polar axis concentrator is seen to be less sensitive to loss of diffuse radiation than the concentrator with the E.W. axis; the reason lies in the reduced average incidence angle for polar axis tracking For very clear climates, $\bar{K}_h$ = .7, a high concentration collector with E.W. axis receives only 73% of the radiation available to a fixed flat plate, where as a high

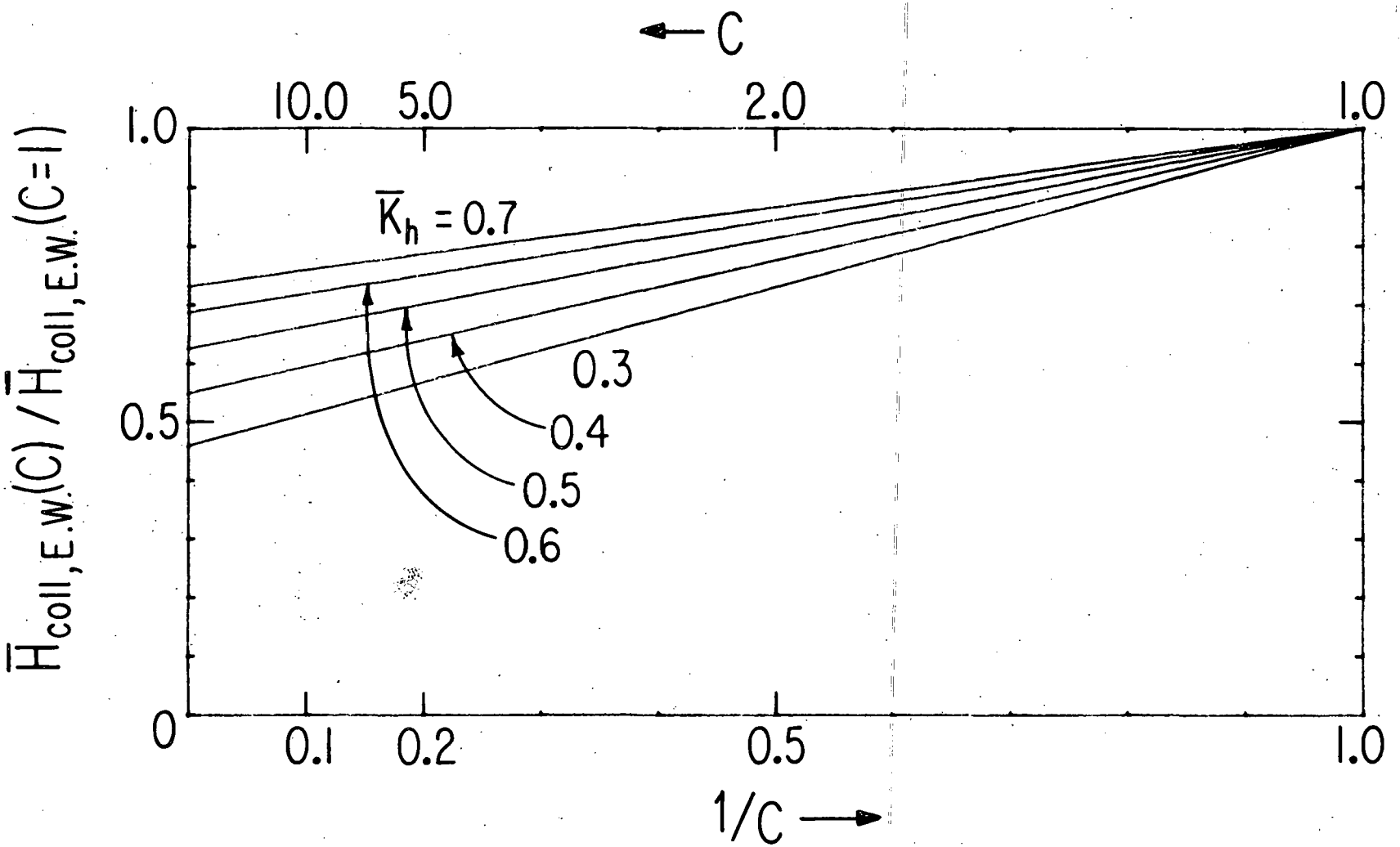

Fig. 9a. Radiation availability for concentrator with east-west axis at equinox, as function of concentration ratio C, for different values of clearness index $\bar{K}_h$.

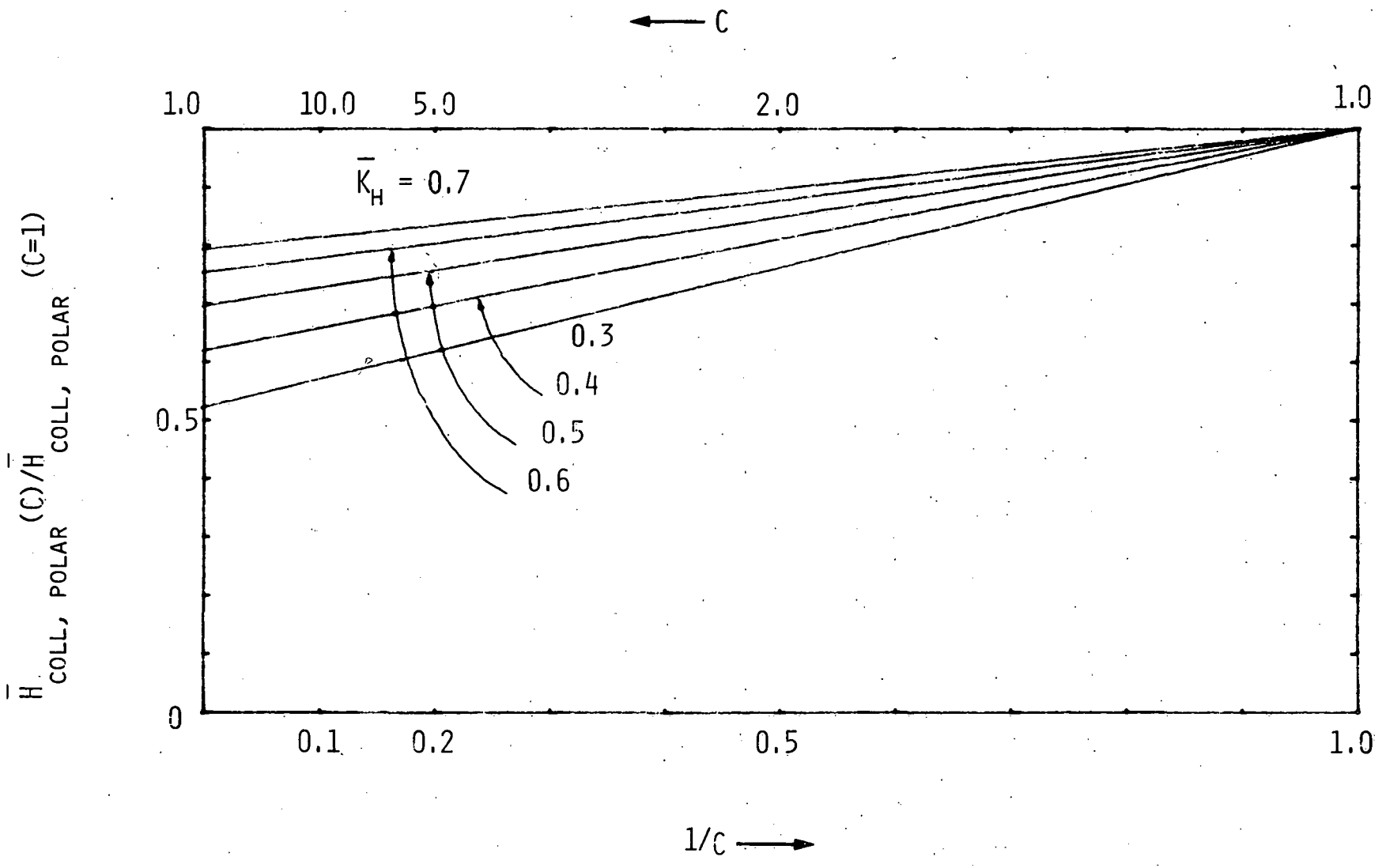

Fig. 9b. Radiation availability for concentrator with polar axis at equinox, as a function of concentration ratio C, for different values of clearness index $\bar{K}_h$.

concentration collector with polar axis receives 80% of the radiation available to a polar axis tracking flat plate. For cloudy climates, $\bar{K}_h$ = .3, the corresponding ratios drop to 46% for the E.W. axis and to 52% for the polar axis.

Table X and Figs. 9a) and b) provide general rules of thumb about the effects of tracking and concentration. For example for $\bar{K}_h$ = .5, typical of average cloudiness, Table X indicates that tracking enhances the energy availability for flat plates by about 25%, while Fig. 9b) shows that high concentration reduces the energy availability by about 30%. Therefore the improvement in average incidence angle brought about by polar axis tracking nearly compensates for the loss of diffuse radiation associated with high concentration.

Acknowledgments

Throughout the course of this work we have benefited from discussions with many of our colleagues. In particular we should like to thank Dr. S. A. Klein for valuable comments, and Mr. H. W. Gaul and Dr. K. H. Macomber for checking some of the results.

References

1. B.Y. H. Liu and R. C. Jordan, "A Rational Procedure for Predicting the Long Term Average Performance of Flat-Plate Solar-Energy Collectors", Solar Energy 7, 53 (1963).
2. W.A. Beckman, S.A. Klein, and J.A. Duffie, "Solar Heating Design by the f-chart Method", John Wiley & Sons, New York (1977).
3. For the flat-plate collector this simplification has also been found by S.A. Klein "Calculation of Flat Plate Collector Utilizability", to be publ. in Solar Energy. For the example of the flat plate in our Table VI Klein's method agrees with ours to 1%.
4. H.C. Hottel and A. Whillier, "Evaluation of Flat Plate Solar Collector Performance", Transactions of the Conference on the use of Solar Energy: The Scientific Basis, Vol. II, Part 1, Section A. pp. 74-104 (1955).
5. Grether, D.F., Hunt, A., Wahlig, M., "Results from Circumsolar Radiation Measurements", Proceedings of the Joint Canada-American Conference, ISES, Vol.1, p. 363, 1976.
6. K.R. Reed, "Instrumentation for Measuring Direct and Diffuse Insolation in Testing Thermal Collectors", Optics in Solar Energy Utilization II, SPIE (1976), vol. 85.
7. A preliminary version of this model was presented Sept. 1977: M. Collares-Pereira and A. Rabl, "Simple Procedure for predicting Long Term Average Performance of Nontracking and of Tracking Solar Collectors", proceedings of "Deutsches Sonnenforum", Hamburg 26-28 Sept. 1977, Vol. 1, p. 275.
8. M. Collares-Pereira and A. Rabl, "The Average Distribution of Solar Radiation - Correlations Between Diffuse and Hemispherical and Between Daily and Hourly Insolation Values", June 1977, to be published in Solar Energy, Vol. 21, 1977.
9. M. Collares-Pereira and A. Rabl, "Derivation of Method for Predicting Long Term Average Energy Delivery of Solar Collectors" - in preparation. The functions R_d and R_h are integrals over time of day of the conversion factors r_d and r_h between daily and instantaneous insolation values of Ref. 8, convoluted over incidence angle factors.

10. J.E. Hill and E. R. Streed, "A Method of Testing for Rating Solar Collectors Based on Thermal Performance", Solar Energy 18, 421 (1976).
F. F. Simon, "Flat Plate Solar Collector Performance Evaluation with a Solar Simulator as a Basis for Collector Selection and Performance Prediction", Solar Energy 18, 451 (1976).
11. H. Tabor, "Testing of Solar Collectors", Solar Energy 20, 293 (1978).
12. J. A. Duffie and W. A. Beckman, "Solar Energy Thermal Processes", John Wiley & Sons, New York, 1974.
F. Kreith and J. F. Kreider. "Principles of Solar Engineering". McGraw-Hill Book Co., New York (1978).
13. F. de Winter, "Heat Exchanger Penalties in Double-Loop Solar Water Heating Systems", Solar Energy 17, 335 (1976).
14. G. R. Mather and D. C. Beekley, "Performance of Evacuated Tubular Collector Using Nonimaging Reflectors", Proceedings of "Sharing the Sun", Vol. 2, p. 64, Winnepeg, Aug. 1976.
G. R. Mather, Jr. and D. C. Beekley, Analysis and Experimental Tests of High Performance Tubular Solar Collectors, ISES Conference in Los Angeles, Calif. (July 1975).
15. A. Rabl, "Comparison of Solar Concentrators", Solar Energy 18, 93 (1976).
16. A. Rabl, "Concentrating Collectors", in Solar Energy Handbook, W. C. Dickinson and P. N. Cheremisinoff, Editors, Marcel Dekker, Inc., New York, Basel (1978).
17. R. Winston, "Solar Concentrators of a Novel Design", Solar Energy 16, 89 (1974).
18. A. Rabl, "Optical and Thermal Analysis of Concentrators", Solar Thermal Concentrating Collector Technology Symposium, Denver, Co., 14 and 15 June 1978.
19. J. Leonard, "Linear Concentrating Solar Collectors -- Current Technology and Applications", Solar Thermal Concentrating Collector Technology Symposium, Denver, Co., 14 and 15 June 1978.
V. E. Dudley and R. M. Workhoven, "Summary Report: Concentrating Solar Collector Test Results Collector Module Test Facility", Sandia report SAND 78-0815 (1978).

20. R. Bingham, Final Report for Contract 31-109-38-3805, General Electric Space Division (1977).

21. The long term average performance of a CPC has also been calculated by R. L. Cole, "Long Term Average Performance Predictions for Compound Parabolic Concentrator", Proc. 1977 Meeting U.S. Section Int. Solar Energy Soc., Orlando, Florida, June 1977, p. 36-6.

22. E. C. Boes, H. E. Anderson, I. J. Hall, R. R. Prairie and R. T. Stromberg, "Availability of Direct, Total, and Diffuse Solar Radiation to Fixed and Tracking Collectors in the USA", Sandia Laboratories Report SAND 77-0885, August 1977.

23. D. L. Evans, "Simplified Solar Irradiation Data Based on the Aerospace Insolation Data Base", Arizona State University Report ERC-R-77077, for SANDIA Laboratories Contract No. 02-7850, 1977.

24. K. C. Brown, Solar Energy Research Institute, private communication.

APPENDIX A.

Extraterrestrial Insolation

The extraterrestrial radiation H_o is given by [12]

$$H_o = \frac{T}{\pi} I_o \left[1 + 0.033 \cos\left(\frac{2\pi n}{365.24}\right)\right] \cos\lambda \cos\delta (\sin\omega_s - \omega_s \cos\omega_s) \quad \text{(A-1)}$$

with T = length of day = 24 hr.

I_o = 1353 ω/m^2 = solar constant

n = day of year (starting 1 January)

λ = geographic latitude

ω_s = arccos [-tan λ tan δ] = sunset hour angle

and δ = solar declination given by

$$\sin\delta = 0.3979 \sin\gamma \quad \text{(A-2)}$$

(Note 0.3979 = sin 23.45°)

In the approximation of a circular orbit of the earth γ is

$$\gamma \approx \gamma_o = \frac{2\pi(n+284)}{365.24} \quad ; \quad \text{(A-3)}$$

for greater accuracy the expression

$$\gamma[\text{radians}] = \gamma_o + 0.00713 \sin\gamma_o + 0.032680 \cos\gamma_o \quad \text{(A-4)}$$

$$-0.000318 \sin 2\gamma_o + 0.000145 \cos 2\gamma_o$$

is recommended by R. L. Hulstrom and M. Imamura, "Definition Study for Photovaltaic Residential Prototype Systems", Final Report, Martin Marietta report MCR-76-394, September 1976; Appendix A.

APPENDIX B.

Long-term Average Values of Insolation, Clearness Index, and Ambient Temperature (adapted from Ref. 2)*

	JAN	FEB	MAR	APR	MAY	JUNE	JULY	AUG	SEP	OCT	NOV	DEC
ALBUQUERQUE NM (LAT. 35.0)												
$\bar{H}_h$ MJ/m²	12.88	16.31	21.41	26.35	28.77	30.90	28.86	26.60	23.67	18.69	14.13	11.75
$\bar{K}_h$	.71	.71	.73	.74	.73	.75	.72	.72	.75	.75	.74	.71
$\bar{T}_a$ C	1.0	4.0	7.0	12.0	17.0	22.0	25.0	23.0	20.0	13.0	6.0	1.0
BLUE HILL MA (LAT. 42.1)												
$\bar{H}_h$ MJ/m²	6.52	8.99	12.71	15.85	19.70	21.62	20.91	18.15	14.72	10.41	6.61	5.39
$\bar{K}_h$	.47	.47	.49	.47	.50	.52	.52	.51	.51	.49	.44	.44
$\bar{T}_a$ C	-3.0	-3.0	1.0	7.0	13.0	18.0	21.0	20.0	16.0	11.0	5.0	-1.0
DALLAS TX (LAT. 32.5)												
$\bar{H}_h$ MJ/m²	9.67	12.85	16.49	19.01	21.81	24.91	24.62	22.52	19.17	15.20	10.93	9.25
$\bar{K}_h$	.49	.53	.54	.53	.55	.61	.61	.60	.59	.58	.53	.51
$\bar{T}_a$ C	7.0	10.0	13.0	19.0	23.0	28.0	30.0	30.0	26.0	20.0	13.0	9.0
DENVER CO (LAT. 39.4)												
$\bar{H}_h$ MJ/m²	10.68	14.15	18.25	21.73	24.37	27.38	26.50	24.79	20.68	15.49	10.97	9.13
$\bar{K}_h$	.69	.69	.67	.63	.62	.66	.66	.68	.69	.69	.66	.65
$\bar{T}_a$ C	-1.0	.0	3.0	9.0	14.0	19.0	23.0	22.0	17.0	11.0	4.0	.0
LEMONT IL (LAT. 41.4)												
$\bar{H}_h$ MJ/m²	7.15	9.70	13.63	16.31	20.78	23.13	22.04	20.32	16.06	11.08	6.57	5.48
$\bar{K}_h$	.50	.50	.51	.48	.53	.56	.55	.57	.55	.51	.43	.43
$\bar{T}_a$ C	-3.0	-2.0	3.0	10.0	16.0	21.0	24.0	23.0	19.0	13.0	5.0	-1.0
MEMPHIS TN (LAT. 35.0)												
$\bar{H}_h$ MJ/m²	8.04	11.18	15.03	19.68	23.19	24.66	24.41	22.40	18.50	14.82	9.96	7.70
$\bar{K}_h$	.44	.48	.51	.55	.59	.60	.61	.61	.59	.60	.52	.46
$\bar{T}_a$ C	5.0	7.0	11.0	17.0	22.0	26.0	28.0	27.0	23.0	17.0	10.0	6.0
MIAMI FL (LAT. 25.5)												
$\bar{H}_h$ MJ/m²	14.34	17.40	20.53	22.75	23.08	22.21	22.46	21.24	18.69	16.27	14.80	13.34
$\bar{K}_h$	.61	.62	.63	.61	.59	.55	.57	.56	.55	.56	.60	.60
$\bar{T}_a$ C	19.0	19.0	21.0	23.0	25.0	27.0	27.0	28.0	27.0	25.0	22.0	20.0
NEW YORK NY (LAT. 40.5)												
$\bar{H}_h$ MJ/m²	5.44	8.33	12.14	15.45	18.09	19.68	19.22	16.29	13.86	10.13	6.15	4.81
$\bar{K}_h$	.37	.41	.45	.45	.46	.48	.48	.45	.47	.46	.38	.36
$\bar{T}_a$ C	.0	1.0	5.0	11.0	17.0	22.0	25.0	24.0	20.0	15.0	9.0	2.0
SALT LAKE CITY UT (LAT. 40.5)												
$\bar{H}_h$ MJ/m²	6.82	10.72	14.82	20.06	23.87	26.00	25.96	23.07	18.67	13.23	8.54	6.11
$\bar{K}_h$	.46	.53	.55	.59	.61	.63	.64	.64	.63	.60	.53	.46
$\bar{T}_a$ C	-1.0	1.0	4.0	10.0	15.0	19.0	25.0	24.0	18.0	11.0	4.0	.0
SAN DIEGO CA (LAT. 32.4)												
$\bar{H}_h$ MJ/m²	11.10	14.36	17.92	19.43	20.64	21.35	22.90	20.89	18.67	15.11	11.89	10.26
$\bar{K}_h$	.57	.59	.59	.54	.52	.52	.57	.56	.58	.58	.57	.56
$\bar{T}_a$ C	12.0	13.0	14.0	15.0	17.0	18.0	20.0	21.0	21.0	18.0	15.0	13.0
WICHITA KS (LAT. 37.4)												
$\bar{H}_h$ MJ/m²	9.29	11.97	15.99	19.76	22.78	25.20	24.41	22.57	18.71	14.40	10.26	8.29
$\bar{K}_h$	.56	.55	.56	.57	.58	.61	.61	.62	.61	.61	.58	.54
$\bar{T}_a$ C	.0	2.0	6.0	14.0	19.0	24.0	27.0	26.0	21.0	15.0	7.0	1.0

*After completion of this work we learned that Ref. 2 lists the average temperature during day and night, not the average daytime temperature; the difference is on the order of 1 to 3°C in most cases.

APPENDIX C.

Specification of Instantaneous Efficiency

The instantaneous collector efficiency[10,11] serves as basis of the calculation and must be specified in a clear and unambiguous manner. We briefly review the most important characteristics.

1. SPECIFICATION OF INSOLATION

Traditionally the efficiency of flat plate collectors has been referred to hemispherical (also called global or total) irradiance I_h, and that of collectors with high concentration to beam (also called direct) irradiance I_b; this has been assumed as the basis of the present paper. For the intermediate case of concentrators with low concentration no clear consensus has yet emerged. Within the framework of this paper it has been most convenient to base the efficiency of such collectors on radiation within the acceptance angle. If the efficiency data have not been presented in this form correction factors must be applied. Fortunately the conversion from one insolation base to another is straight forward and involves only a multiplicative factor. To find this factor let us add subscripts to the efficiency. If q_{out} is the collector output [in W] relative to net collector aperture area A, then the efficiency with respect to hemispherical irradiance I_h (pyranometer)

$$\eta_h = \frac{q_{out}}{A\ I_h} \tag{C-1}$$

while the efficiency with respect to beam I_b (pyreheliometer)

$$\eta_b = \frac{q_{out}}{A\ I_b} \tag{C-2}$$

The conversion from one to the other is therefore

$$\eta_b = \eta_h \frac{I_h}{I_b} = \eta_h \left(1 + \frac{I_d}{I_b}\right) \tag{C-3}$$

where $I_d = I_h - I_b$ is the diffuse component. Since efficiency measurements should always be done under clear sky, the ratio I_d/I_b of diffuse over beam is about 0.1 to 0.15. This means that the efficiency curve of a collector is at least 10% higher when stated in terms of beam rather than in terms of hemispherical radiation. For collectors with low concentration $1 < C \leq 10$, e.g. CPC and V-trough which accept significant fraction, 1/C of the diffused component,[15,16], the efficiency relative to the irradiance

$$I_c = I_b + \frac{1}{C} I_d \qquad \text{(C-6)}$$

within the acceptance angle

$$\eta_c = \frac{q_{out}}{A\ I_c} \qquad \text{(C-7)}$$

the conversion factor from η_h to η_c is given by

$$\eta_c = \eta_h \frac{1 + \frac{I_d}{I_b}}{1 + \frac{I_d}{C\ I_b}} \qquad \text{(C-8)}$$

and the conversion from η_c to η_b is

$$\eta_c = \eta_b \cdot \frac{1}{1 + \frac{I_d}{C \cdot I_b}} \qquad \text{(C-9)}$$

2. REFERENCE TEMPERATURE

Several collector temperatures can serve as reference for stating the efficiency, the most useful being

T_r = average collector receiver surface temperature

T_{in} = fluid inlet temperature

T_{out} = fluid outlet temperature

$T_f = (T_{in} + T_{out})/2$ = average fluid temperature

To a very good approximation only the difference between the collector temperature and

T_a = ambient temperature

matters. The heat loss coefficient or U-value U[in $W/m^2°C$] is defined relative to collector aperture area A as

$$U = \frac{q_\ell}{A(T_r - T_a)} \qquad \text{(C-9)}$$

where q_ℓ is the heat loss [in W]. Strictly speaking U is not constant; but its dependence on temperature, wind and other environmental factors is fairly weak, and good approximation is obtained by using an average U-value corresponding to the anticipated operating temperature. For a better approximation we recommend Tabor's parameterization[11]

$$q_\ell = AU_o(T_r - T_a)^p \qquad \text{(C-10)}$$

where p is a collector dependent coefficient, typically in the range 1.1 to 1.3 for nonevacuated collectors and somewhat larger for evacuated collectors.

In terms of U the collector efficiency reads

$$\eta = \eta_o - U(T_r - T_a)/I \qquad \text{(C-11)}$$

if the average receiver surface temperature T_r is given. η_o is the optical efficiency or efficiency at zero heat loss; it has also been called $\tau\alpha$ product in the flat plate literature.

Usually it is more practical to measure the fluid temperature than the receiver surface temperature. In terms of the average fluid temperature T_f the efficiency equals

$$\eta = F'[\eta_o - U(T_f - T_a)/I] \qquad \text{(C-12)}$$

where F' is the heat extraction factor (called collector efficiency factor in Ref.12) given by the ratio

$$F' = \frac{U_{fa}}{U} \qquad \text{(C-13)}$$

of the thermal conductance U_{fa} from fluid to ambient over the thermal conductance from receiver surface to ambient (in this equation both U values must refer to aperture area). If the fluid inlet temperature T_{in} is specified, the efficiency is

$$\eta = F_R[\eta_o - U(T_{in} - T_a)/I] \qquad \text{(C-14)}$$

with the heat removal factor[12]

$$F_R = \frac{\dot{m}c_p}{UA}\left[1 - \exp\left(\frac{-UAF'}{\dot{m}c_p}\right)\right] \qquad \text{(C-15)}$$

$\dot{m}$ is the mass flow rate [kg/s] through the collector and C_p is the fluid heat capacitance [J/Kg °C] at constant pressure. Finally, the dependence of efficiency on fluid outlet temperature T_{out} is given by a modification[13] of Eq (C -14)

$$\eta = \frac{F_R}{\left[1 - \frac{F_R UA}{\dot{m}c_p}\right]}[\eta_o - U(T_{out} - T_a)/I]. \qquad \text{(C-16)}$$

Any of the four expressions for efficiency, (C-11), (C-12) , (C-14) or (C-16) can be used as starting points for the calculation of long term average performance.

3. INCIDENCE ANGLE MODIFIERS AND AVERAGE OPTICAL EFFICIENCY

Measurements of instantaneous efficiency are usually carried out and reported at normal or nearly normal incidence. In actual operation, on the other hand, the incidence angle on any collector with less than full 2 axis tracking will vary over the course of the day and the year.

Usually the optical efficiency decreases with large incidence angles because of increased reflection from cover glazing and because of geometric factors. This effect could be described by an incidence angle modifier $F(\theta_{EW},\theta_{NS})$ which multiplies the optical efficiency η_o[9]. It is however much simpler to replace η_o by its long term average $\bar{\eta}_o$. In practice $\bar{\eta}_o$ should be determined by measuring the average day long efficiency on a clear day from $t=t_{c-}$ until $t=t_{c+}$

$$\bar{\eta}_o = \left. \frac{\int_{tc-}^{tc+} dt \, \frac{q_{out}(t)}{A}}{\int_{tc-}^{tc+} dt \, I(t)} \right|_{T_r=T_a} \qquad \text{(C-17a)}$$

with average receiver temperature T_r kept as close as possible to ambient T_a to minimize heat loss. The turn-on and turn-off times t_{c-} and t_{c+} for this test should be representative of average operating periods for the collector in question. If the condition $T_r = T_a$ cannot be satisfied, one must correct Eq. (C-17a) by adding the daily total heat loss calculated from the known U-value as

$$\bar{\eta}_o = \frac{\int_{tc-}^{tc+} dt \left\{ \frac{q_{out}(t)}{A} + U[T_r(t)-T_a(t)] \right\}}{\int_{-tc-}^{tc+} dt \quad I(t)} \qquad \text{(C-17b)}$$

if the receiver temperature $T_r(t)$,

and as

$$\bar{\eta}_o = \frac{\int_{tc-}^{tc+} dt \left\{ \frac{q_{out}(t)}{AF'} + U[T_f(t)-T_a(t)] \right\}}{\int_{tc-}^{tc+} dt \quad I(t)} \qquad \text{(C-17c)}$$

if the average fluid temperature $T_f(t)$ has been monitored.

The precise values of t_{c-} and t_{c+} used for this measurement are not critical. For example a flat plate collector will typically operate for about 7 hours per day. If instead 6 or 8 hours were used for measuring $\bar{\eta}_o$ the result would differ by less than 1%.

Table I. Function R_h and R_d for Flat Plate Collector

a) tilt β = latitude λ, azimuth $\phi = 0$

$$R_h = \frac{1}{d}\left\{\left[\frac{1}{\cos\lambda} + \frac{\rho}{2}(1-\cos\lambda)\right]\left[a\sin\omega_c + \frac{b}{2}(\sin\omega_c\cos\omega_c + \omega_c)\right] - \frac{\rho}{2}(1-\cos\lambda)\cos\omega_s\,[a\,\omega_c + b\sin\omega_c]\right\}$$

$$R_d = \frac{1}{d}\left\{\left[\frac{1}{\cos\lambda} - \frac{1}{2}(1+\cos\lambda)\right]\sin\omega_c + \left[\frac{1}{2}(1+\cos\lambda)\cos\omega_s\right]\omega_c\right\}$$

b) tilt $\beta \neq$ latitude λ, azimuth $\phi = 0$

$$R_h = \frac{1}{d}\left\{\left[\frac{\cos(\lambda-\beta)}{\cos\lambda} + \frac{\rho}{2}(1-\cos\beta)\right]\left[a\sin\omega_c + \frac{b}{2}(\sin\omega_c\cos\omega_c + \omega_c)\right] - \left[\frac{\cos(\lambda-\beta)}{\cos\lambda}\cos\omega_s' + \frac{\rho}{2}(1-\cos\beta)\cos\omega_s\right]\left[a\,\omega_c + b\sin\omega_c\right]\right\}$$

$$R_d = \frac{1}{d}\left\{\left[\frac{\cos(\lambda-\beta)}{\cos\lambda} - \frac{1}{2}(1+\cos\beta)\right]\sin\omega_c - \left[\frac{\cos(\lambda-\beta)}{\cos\lambda}\cos\omega_s' - \frac{1}{2}(1+\cos\beta)\cos\omega_s\right]\omega_c\right\}$$

c) tilt $\beta \neq$ latitude λ, azimuth $\phi \neq 0$

convert from β and ϕ (with respect to horizontal and vertical) to β_o and ϕ_o (with respect to equatorial plane and polar axis) by means of

$$\sin\beta_o = \cos\beta\sin\lambda - \sin\beta\cos\lambda\cos\phi$$

and

$$\tan\phi_o = \frac{\sin\beta\sin\phi}{\cos\beta\cos\lambda + \sin\beta\sin\lambda\cos\phi}$$

Table I. continued:

$$R_h = \frac{1}{2d}\left\{\left[\frac{\cos\beta_o\cos\phi_o}{\cos\lambda} + \frac{\rho}{2}(1-\cos\beta)\right]\left[a(\sin\omega_{c+}-\sin\omega_{c-}) + \frac{b}{2}(\sin\omega_{c+}\cos\omega_{c+} - \sin\omega_{c-}\cos\omega_{c-} + \omega_{c+} - \omega_{c-})\right] - \frac{\cos\beta_o\sin\phi_o}{\cos\lambda}\left[a(\cos\omega_{c+} - \cos\omega_{c-}) + \frac{b}{2}(\cos^2\omega_{c+} - \cos^2\omega_{c-})\right] + \tan\delta\left[\frac{\sin\beta_o}{\cos\lambda} + \frac{\rho}{2}(1-\cos\beta)\tan\lambda\right]\left[a(\omega_{c+} - \omega_{c-}) + b(\sin\omega_{c+} - \sin\omega_{c-})\right]\right\}$$

$$R_d = \frac{1}{2d}\left\{\left[\frac{\cos\beta_o\cos\phi_o}{\cos\lambda} - \frac{1}{2}(1+\cos\beta)\right](\sin\omega_{c+} - \sin\omega_{c-}) - \frac{\cos\beta_o\sin\phi_o}{\cos\lambda}(\cos\omega_{c+} - \cos\omega_{c-}) + \tan\delta\left[\frac{\sin\beta_o}{\cos\lambda} - \frac{1}{2}(1+\cos\beta)\tan\lambda\right](\omega_{c+} - \omega_{c-})\right\}$$

Table II.

Functions R_d and R_h for concentrators with fixed aperture, e.g., compound parabolic concentrator (CPC)

a) tilt β = latitude λ, azimuth $\phi = 0$

$$R_h = \frac{1}{d \cos \lambda} \left\{ a \sin \omega_c + \frac{b}{2} (\sin \omega_c \cos \omega_c + \omega_c) \right\}$$

and

$$R_d = \frac{1}{d} \left\{ \left[\frac{1}{\cos \lambda} - \frac{1}{C} \right] \sin \omega_c + \frac{\cos \omega_s}{C} \omega_c \right\}$$

b) tilt $\beta \neq$ latitude λ, azimuth $\phi = 0$

$$R_h = \frac{\cos (\lambda-\beta)}{d \cos \lambda} \left\{ (a - b \cos \omega_s') \sin \omega_c - a \cos \omega_s' \omega_c + \frac{b}{2} (\sin \omega_c \cos \omega_c + \omega_c) \right\}$$

and

$$R_d = \frac{1}{d} \left\{ \left[\frac{\cos (\lambda-\beta)}{\cos \lambda} - \frac{1}{C} \right] \sin \omega_c + \left[\frac{\cos \omega_s}{C} - \frac{\cos(\lambda-\beta)}{\cos \lambda} \cos \omega_s' \right] \omega_c \right\}$$

TABLE III.

Functions R_h and R_d for a collector which tracks about East-West axis

$$R_h = \frac{1}{d \cos \lambda} \int_0^{\omega_c} d\omega \quad (a + b \cos \omega) \quad \sqrt{\cos^2 \omega + \tan^2 \delta}$$

$$R_d = \begin{cases} \dfrac{1}{d \cos \lambda} \displaystyle\int_0^{\omega_c} d\omega \quad \sqrt{\cos^2 \omega + \tan^2 \delta} & \text{for high concentration } C \gtrsim 10 \\ \dfrac{1}{d \cos \lambda} \displaystyle\int_0^{\omega_c} d\omega \quad \left[\sqrt{\cos^2 \omega + \tan^2 \delta} - \frac{\cos \lambda}{C} \quad (\cos \omega - \cos \omega_s) \right] & \text{for low concentration } C \lesssim 10 \end{cases}$$

to evaluate these integrals one can use Simpson's rule or elliptic integrals, as explained below.

Simpson's rule with one step will be adequate in most cases (error < 3%); for greater accuracy two steps can be used.

$$\int_{x_o}^{x_o + 2\Delta x} f(x)dx \approx \frac{\Delta x}{3} [f(x_o) + 4 f (x_o + \Delta x) + f (x_o + 2\Delta x)]$$

In terms of elliptic integrals R_h and R_d are

$$R_h = \frac{1}{d \cos \lambda \cos \delta} \left\{ a \, E \left(\omega_c, \frac{\pi}{2} - \delta\right) + \frac{b}{2} \left[\sin \omega_c \sqrt{1 - \cos^2 \delta \sin^2 \omega_c} + \frac{\arcsin (\cos \delta \sin \omega_c)}{\cos \delta} \right] \right\}$$

Table III. continued:

and

$$R_d = \begin{cases} \dfrac{E\left(\omega_c, \frac{\pi}{2} - \delta\right)}{d \cos\lambda \cos\delta} & \text{for high concentration} \\ \dfrac{E\left(\omega_c, \frac{\pi}{2} - \delta\right)}{d \cos\lambda \cos\delta} - \dfrac{\sin\omega_c - \omega_c \cos\omega_s}{Cd} & \text{for low concentration} \end{cases}$$

where $E(\omega_c, \frac{\pi}{2} - \delta)$ is an elliptic integral of the second kind

$$E(\phi,\alpha) = \int_o^{\phi} d\theta \, (1 - \sin^2\alpha \sin^2\theta)^{1/2}$$

which is tabulated, for example on pp. 616-618 of "Handbook of Mathematical Functions", M. Abramovitz and I. A. Stegun, Dover Publications, Inc., New York 1965.

TABLE IV.

Functions R_h and R_d for collector which tracks about North-South axis

a) tilt of tracking axis β = latitude λ (polar mount)

$$R_h = \frac{a\omega_c + b \sin \omega_c}{d \cos \lambda}$$

and

$$R_d = \begin{cases} \dfrac{\omega_c}{d \cos \lambda} & \text{for high concentration} \\ \dfrac{\omega_c}{d \cos \lambda} - \dfrac{\sin \omega_c - \omega_c \cos \omega_s}{C\, d} & \text{for low concentration} \end{cases}$$

b) tilt of tracking axis $\beta \neq$ latitude λ

$$R_h = \frac{1}{d \cos \lambda} \int_o^{\omega_c} d\omega\, (a + b \cos \omega)\, g(\omega)$$

$$\text{with } g(\omega) = \sqrt{\sin^2 \omega + [\cos(\lambda-\beta)\cos \omega + \tan \delta \sin(\lambda-\beta)]^2}$$

and

$$R_d = \begin{cases} \dfrac{1}{d \cos \lambda} \displaystyle\int_o^{\omega_c} d\omega\, g(\omega) & \text{for high concentration} \\ \dfrac{1}{d \cos \lambda} \displaystyle\int_o^{\omega_c} d\omega\, g(\omega) - \dfrac{\sin \omega_c - \omega_c \cos \omega_s}{C\, d} & \text{for low concentration.} \end{cases}$$

The integrals can be evaluated by Simpson's rule. See Table III.

TABLE V.

Functions R_h and R_d for collector with 2-axis tracking

$$R_h = \frac{a\omega_c + b \sin \omega_c}{d \cos \lambda \cos \delta}$$

and

$$R_d = \begin{cases} \dfrac{\omega_c}{d \cos \lambda \cos \delta} & \text{for high concentration} \\ \dfrac{\omega_c}{d \cos \lambda \cos \delta} - \dfrac{\sin \omega_c - \omega_c \cos \omega_s}{C\, d} & \text{for low concentration} \end{cases}$$

TABLE VI - Collector parameters and energy collected
15 February in New York at 50°C

	Flat Plate	CPC evacuated	Parabolic trough E.W. tracking axis	Parabolic trough polar tracking axis	Two axis tracker
$\bar{\eta}_0$	.75	.6	.65	.65	.65
$U[W/m^2C]$	4	.8	.7	.7	.2
C	1	1.5	20	20	500
F'	.9	.99	.95	.95	.9
t_c (hrs from noon)	3.934	4.651	5.234	5.234	5.234
R_h	1.626	1.723	1.874	2.377	2.441
R_d	.783	1.089	1.932	2.549	2.617
$R=R_d/R_h$	.481	.632	1.031	1.072	1.072
$\bar{H}_{coll}[M\ J/m^2]$ Eq. II-1	10.616	10.278	8.385	10.274	10.550
X(Eq. III-1 and III-2)	.697	.213	.237	.194	.054
$\phi(\bar{K}_h, R, X)$	.470	.807	.856	.881	.966
$(\bar{Q}/A) \Big\vert = \eta_o \phi \bar{H}_{coll}[MJ/m^2]$ T_r=50°C	3.743	4.976	4.667	5.886	6.624
$(\bar{Q}/A) \Big\vert = F' \eta_o \phi \bar{H}_{coll}[MJ/m^2]$ $T_{av.\ fluid}$ = 50°C	3.369	4.926	4.434	5.592	5.962

TABLE VIIa - Some results of the iteration procedure to determine the cut-off time corresponding to the maximum energy (Max.$\bar{Q}_{out}$) collected. Flat plate, tilt = latitude, at $\bar{T}_r$ = 50° in New York in February. Iterations start with $t_c = t_s$ = 5.234 sunset time (hours from noon); decrement Δt_c = 0.1 hr, for the sake of illustration Δt_c has been chosen much smaller than necessary.

Iteration #	(cut-off time) t_c	R_h	R_d	$\bar{H}_{coll}$	X	$\bar{Q}_{out}$
1st	5.234	1.801	.943	11.482	.858	3.405
10th	4.334	1.700	.839	11.027	.739	3.714
14th (Max.$\bar{Q}_{out}$)	3.934	1.626	.783	10.616	.697	3.743
15th	3.834	1.604	.768	10.491	.688	3.738

TABLE VIIb - Some results of the iteration procedure to determine the cut-off time corresponding to the maximum energy (Max.$\bar{Q}_{out}$) collected. Fixed tilt = latitude CPC (1.5X), E.W. tracking axis parabolic trough, polar mount tracking parabolic trough, 2 axis tracker, for New York, and $\bar{T}_r$ = 100°C in February. Due to small heat loss t_c is close to t_s, and omission of iterations (i.e. setting $t_c = t_s$) would affect result for $\bar{Q}$ by less than one percent.

	Iteration #	t_c (cut-off time)	R_h	R_d	$\bar{H}_{coll}$ [MJ/m^2]	X	$\bar{Q}_{out}$ [MJ/m^2]
CPC (1.5X)	1	4.651	1.723	1.089	10.728	.430	3.985
	3 (Max. $\bar{Q}_{out}$)	4.451	1.695	1.062	10.153	.417	3.989
Parabolic trough E.W. Tracking axis	1	5.234	1.874	1.932	8.385	.472	3.955
	5 (Max. $\bar{Q}_{out}$)	4.834	1.827	1.865	8.247	.450	3.970
Parabolic trough Polar tracking axis	1 (Max.$\bar{Q}_{out}$)	5.234	2.377	2.549	10.274	.381	5.151
	2	5.134	2.344	2.500	10.182	.387	5.119
2 axis tracker	1 (Max.$\bar{Q}_{out}$)	5.234	2.441	2.617	10.550	.109	6.391
	2	5.134	2.407	2.567	10.455	.108	6.339

TABLE VIII - Comparison of energy delivery for Lemont, Illinois: daily total cutput for central day of each month, and yearly total, in MJ per m^2 of collector aperture.

LEMONT,IL. LATITUDE 41.40 DEGREES

	JAN	FEB	MAR	APR	MAY	JUN	JUL	AUG	SPT	OCT	NOV	DEC	
INSOLATION	7.150	9.700	13.630	16.310	20.780	23.130	22.040	20.320	16.060	11.080	6.570	5.480	MJ/SQM*DAY
AMBIENT	-3.00	-2.00	3.00	10.00	16.00	21.00	24.00	23.00	19.00	13.00	5.00	-1.00	DEGREE C

COLL.TEMP.-DEG.C — YEAR-MJ/SQM

FLAT PLATE, ETA-0= 0.750 U= 4.0000 WATT/SQM*C TILT = 41.4 DEGREES

TAMB												
	9.625	10.654	12.307	12.432	14.217	14.961	14.594	14.787	13.609	11.349	8.005	7.641	4391.3
75.0	2.905	3.298	4.350	4.558	6.096	7.030	7.134	7.411	6.405	4.512	2.389	2.119	1777.6
150.0	0.0	0.0	0.0	0.0	0.0	0.0	0.0	0.0	0.0	0.0	0.0	0.0	0.0
225.0	0.0	0.0	0.0	0.0	0.0	0.0	0.0	0.0	0.0	0.0	0.0	0.0	0.0
300.0	0.0	0.0	0.0	0.0	0.0	0.0	0.0	0.0	0.0	0.0	0.0	0.0	0.0

CPC FIXED TILT=LAT. ETA-0= 0.600 U= 0.8000 WATT/SQM*C CONCENTRATION = 1.50 THC =34.0

TAMB												
	6.685	7.743	8.948	8.531	8.616	7.982	8.283	9.831	9.851	8.295	5.642	5.119	2908.0
75.0	3.169	3.855	4.843	4.727	7.299	6.965	7.240	8.496	8.111	6.518	4.233	3.837	2557.0
150.0	2.964	4.377	5.193	4.965	5.763	5.639	5.809	6.709	6.227	4.590	3.089	2.874	1815.3
225.0	2.516	3.256	3.902	3.632	4.293	4.413	4.499	5.092	4.728	3.758	2.242	2.164	1378.2
300.0	2.214	2.410	2.911	2.682	3.160	3.288	3.310	3.704	3.525	2.823	1.631	1.592	1012.4

ONE AXIS, EAST-WEST,HORIZONTAL. ETA-0= 0.650 U= 0.7000 WATT/SQM*C

TAMB												
	7.519	7.302	7.323	6.585	8.221	9.377	8.358	8.773	8.014	7.423	5.774	6.009	2776.7
75.0	5.181	5.843	5.246	5.194	6.595	7.718	7.347	7.298	6.715	6.162	4.708	4.927	2269.8
150.0	5.080	4.660	4.649	4.040	4.961	5.695	5.425	5.627	5.331	4.906	3.736	4.003	1764.7
225.0	4.042	3.721	3.690	3.147	3.623	4.209	4.142	4.367	4.217	3.909	2.974	3.228	1359.0
300.0	3.257	2.962	2.915	2.448	2.932	3.271	3.152	3.391	3.309	3.103	2.386	2.615	1068.6

ONE AXIS, SOLAR, TILT=LAT.. ETA-0= 0.650 U= 0.7000 WATT/SQM*C

TAMB												
	9.350	9.804	10.873	9.291	10.994	11.908	11.513	12.281	11.411	9.541	6.591	6.442	3575.5
75.0	7.014	7.527	8.487	7.787	9.342	10.232	9.589	10.776	10.004	8.264	5.317	5.356	3054.9
150.0	5.991	6.257	7.000	6.251	7.468	8.124	7.951	8.784	8.273	6.860	4.509	4.417	2468.8
225.0	4.915	5.094	5.662	4.931	5.812	6.274	6.164	7.002	6.720	5.609	3.650	3.611	1990.7
300.0	3.906	4.097	4.534	3.837	4.612	4.681	4.629	5.431	5.243	4.512	2.939	2.956	1561.0

TWO AXIS TRACKER, ETA-0= 0.650 U= 0.2000 WATT/SQM*C

TAMB												
	8.956	9.296	10.043	9.409	11.595	12.965	12.563	12.639	11.420	9.676	6.965	7.016	3726.1
75.0	8.557	8.848	9.614	8.963	11.106	12.472	11.914	12.198	11.008	9.300	6.644	6.692	3572.3
150.0	8.184	8.393	9.138	8.464	10.503	11.803	11.270	11.577	10.469	8.857	6.312	6.381	3391.8
225.0	7.820	7.990	8.677	7.992	9.919	11.154	10.645	10.973	9.944	8.426	5.991	6.081	3216.6
300.0	7.466	7.598	8.229	7.518	9.353	10.525	10.039	10.385	9.433	8.008	5.682	5.790	3048.9

TABLE IX: $\bar{H}_{coll,\ flat\ plate,\ tracking}/\bar{H}_{coll,\ flat\ plate,\ fixed}$,

ratio of radiation availability for tracking and for fixed flat plate, at equinox.

$\bar{K}_h$ \ λ	0°	10°	20°	30°	40°	50°
.3	1.13	1.13	1.14	1.14	1.15	1.17
.4	1.18	1.18	1.19	1.20	1.21	1.22
.5	1.23	1.23	1.23	1.24	1.25	1.27
.6	1.27	1.27	1.27	1.28	1.29	1.30
.7	1.29	1.29	1.30	1.31	1.32	1.33

TABLE X. Effect of ground reflectance, evaluated by means of the ratio of radiation availability if ground = ρ and if brightness of ground and sky are equal:

$$\frac{\bar{H}_{\text{coll, flat plate, ground = sky}} \left(\omega_s = \frac{\pi}{2}, \omega_c = \frac{\pi}{2}\right)}{\bar{H}_{\text{coll, flat plate, ground = } \rho} \left(\omega_s = \frac{\pi}{2}, \omega_c = \frac{\pi}{2}\right)}$$

λ / $\bar{K}_h$	0°	20°	30°		40°		50°	
	ρ=0.2	ρ=0.2	ρ=0.7	ρ=0.2	ρ=.7	ρ=.2	ρ=0.7	ρ=0.2
.3	1.00	1.01	0.99	1.03	0.99	1.04	0.98	1.06
.4	1.00	1.01	0.99	1.02	0.98	1.03	0.97	1.04
.5	1.00	1.01	0.98	1.01	0.97	1.02	0.96	1.03
.6	1.00	1.00	0.98	1.01	0.97	1.02	0.96	1.02
.7	1.00	1.00	0.98	1.01	0.96	1.01	0.95	1.01

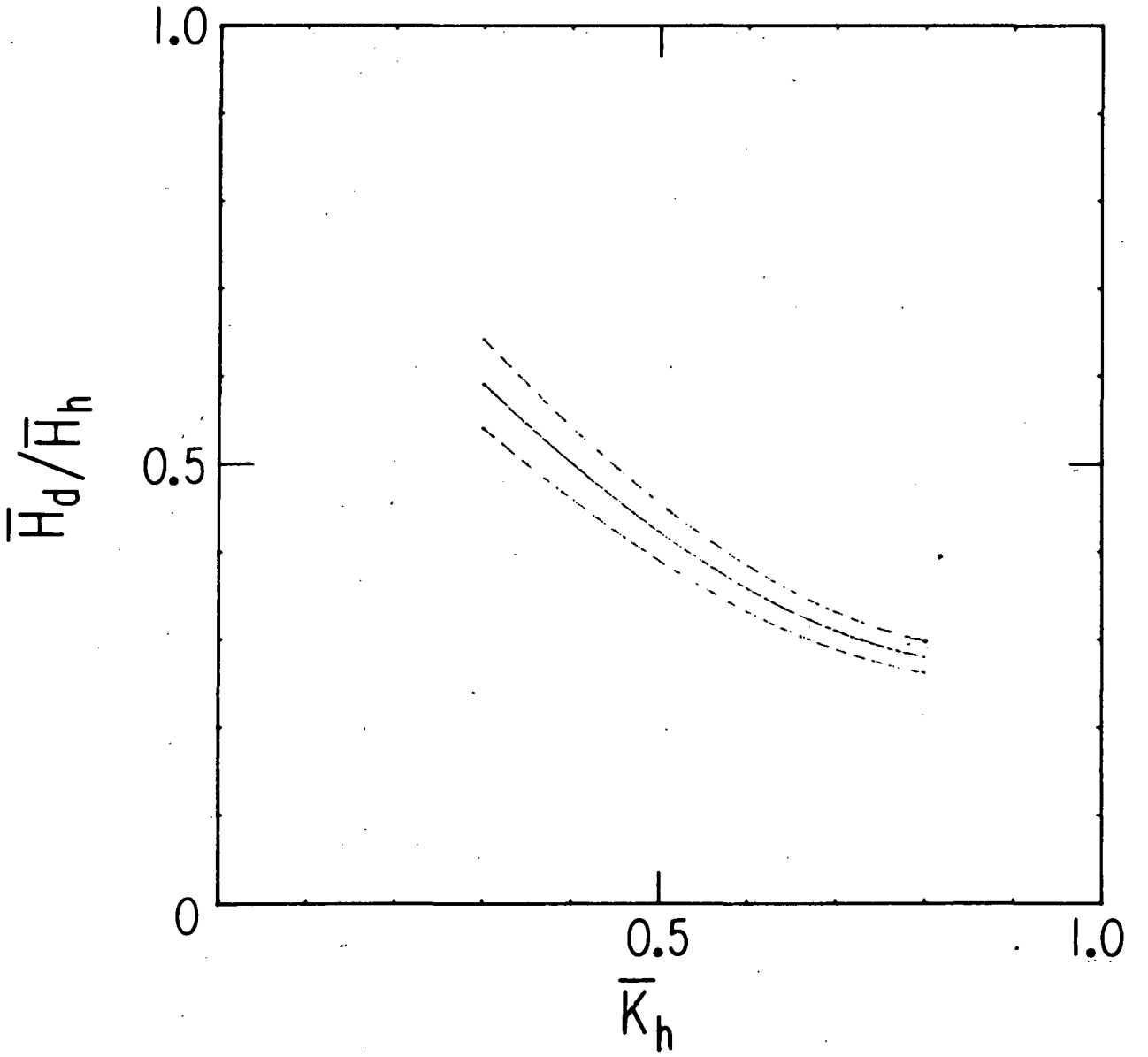

Fig. 1: $\bar{H}_d/\bar{H}_h$ versus $\bar{K}_h$ (Eq. (II-3); the solid line corresponds to $\omega_s = \omega/2$ and the dashed lines correspond to $\omega_s = \frac{\pi}{2} - 0.2$ (bottom).

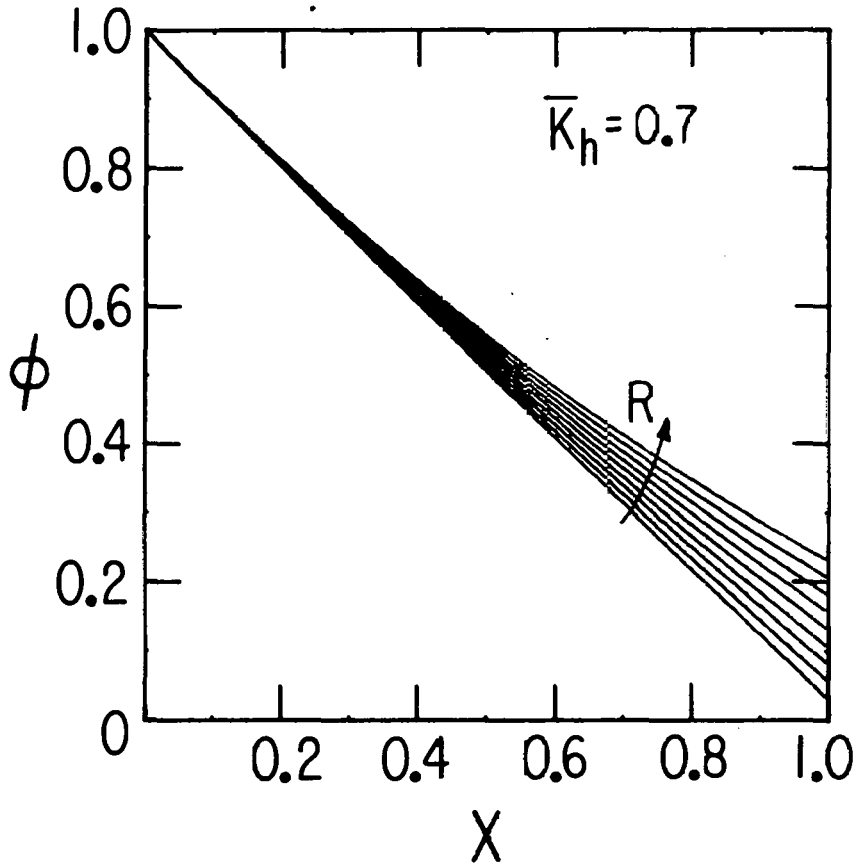

Fig. 2: Utilizability ϕ versus the critical ratio X for $\bar{K}_h = 0.7$ and nine values of R from 0 to 0.8.

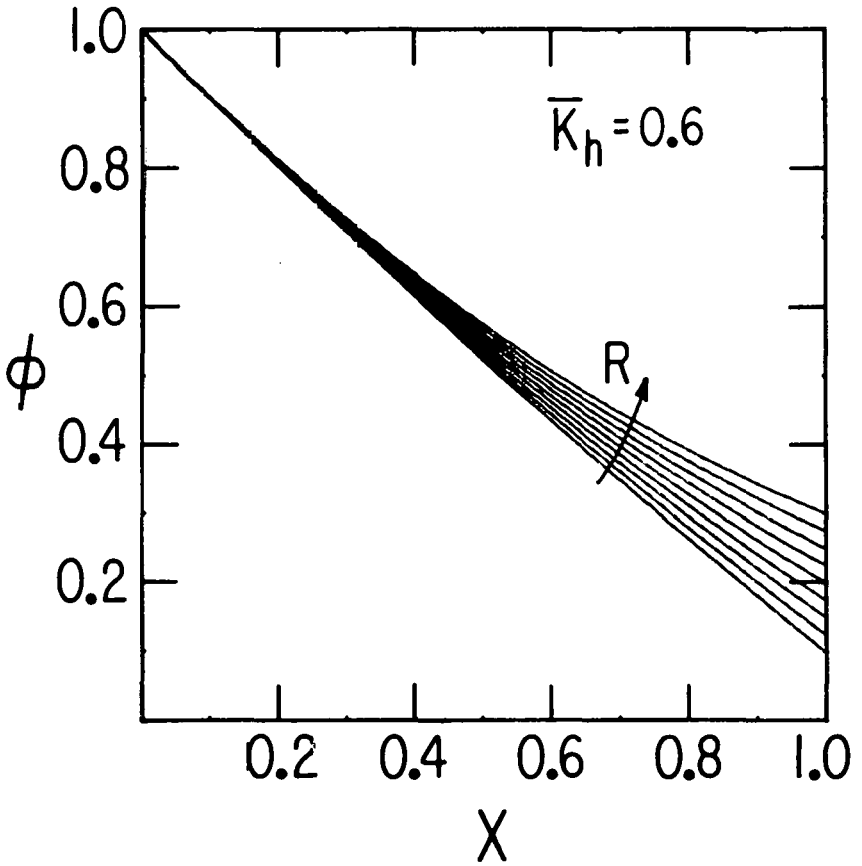

Fig. 3: Utilizability ϕ versus the critical ratio X for $\bar{K}_h = 0.6$ and nine values of R from 0 to 0.8.

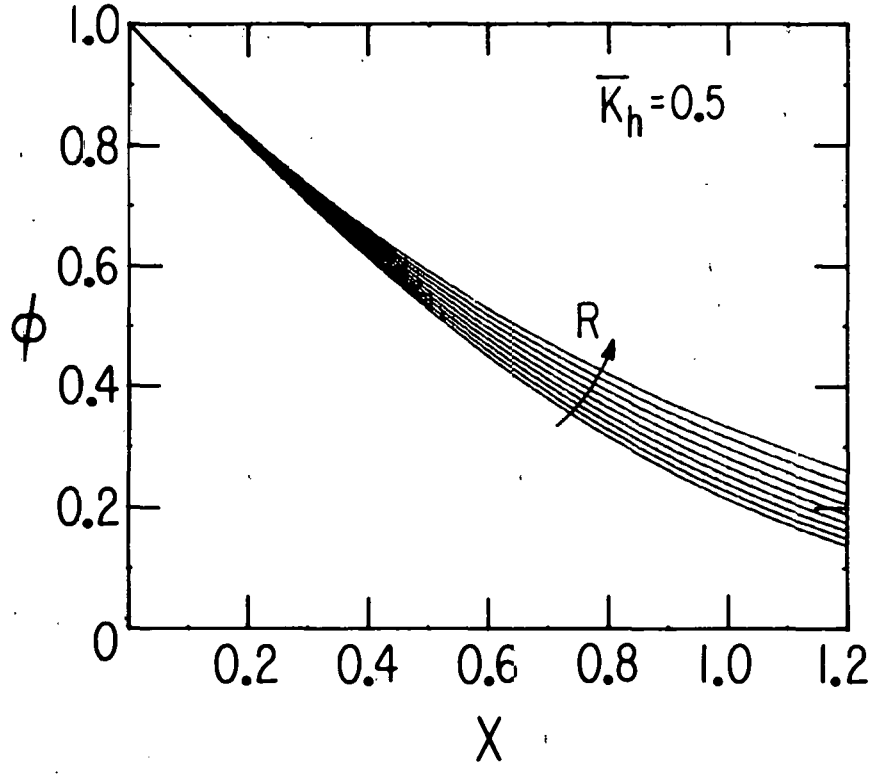

Fig. 4. Utilizability ϕ versus the critical ratio X for $\bar{K}_h$ = 0.5 and nine values of R from 0 to 0.8.

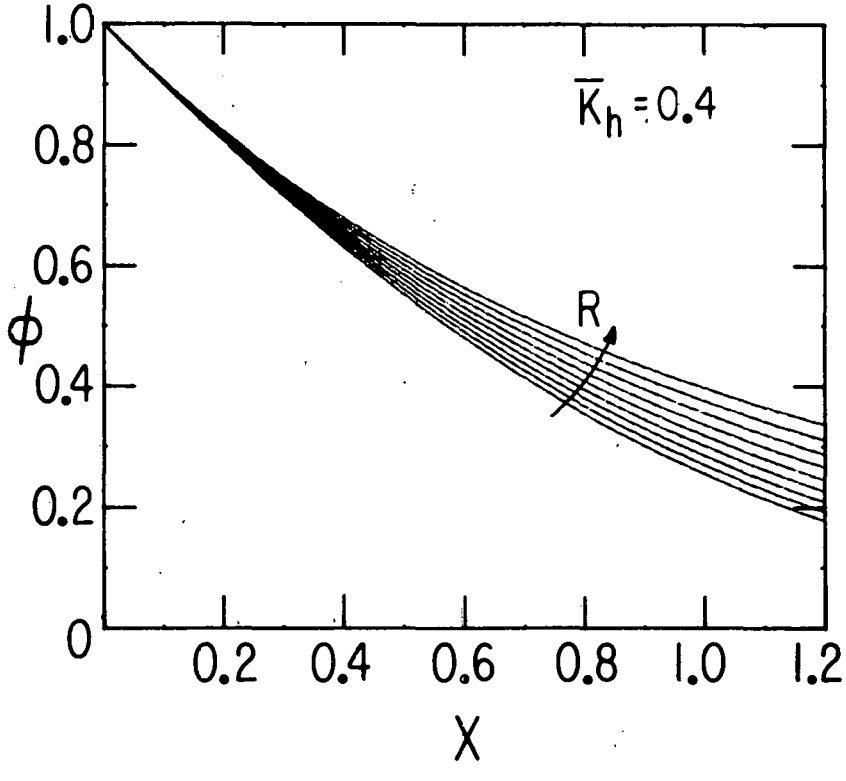

Fig. 5. Utilizability ϕ versus the critical ratio X for $\bar{K}_h$ = 0.4 and nine values of R from 0 to 0.8.

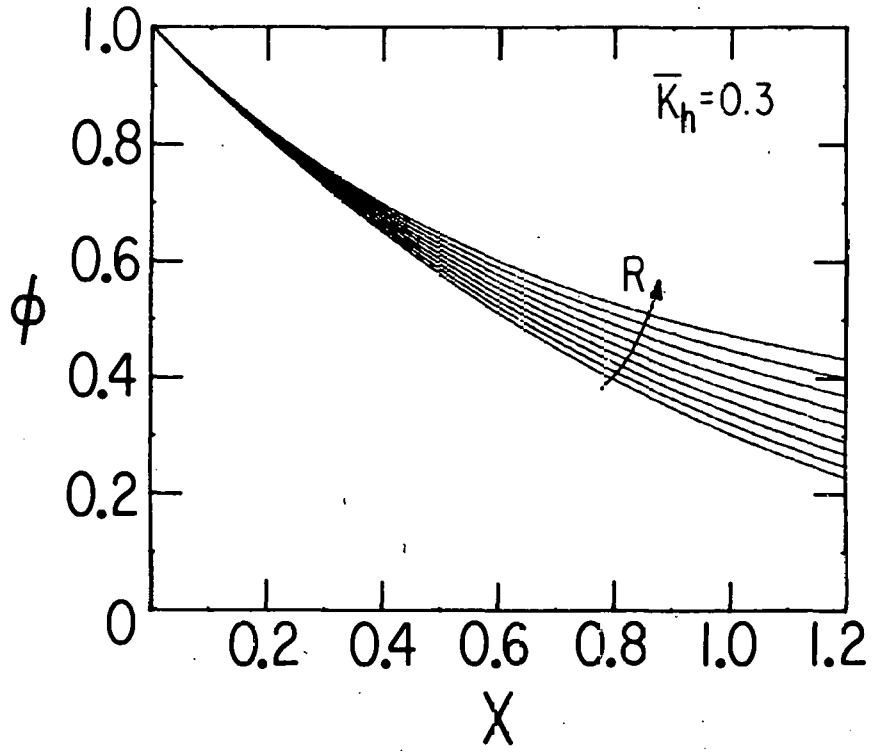

Fig. 6. Utilizability ϕ versus the critical ratio X for $\bar{K}_h$ = 0.3 and nine values of R from 0 to 0.8.

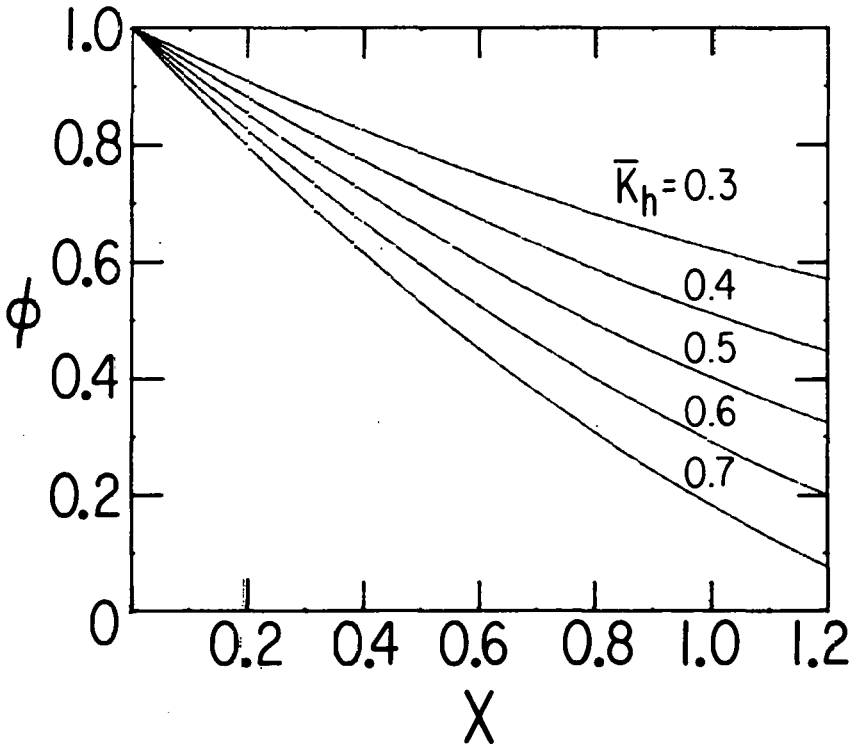

Fig. 7. Utilizability ϕ versus the critical ratio X for collectors with high values of concentration and five $\bar{K}_h$, from 0.3 to 0.7.

Distribution for ANL-78-67

Internal:

J. P. Ackerman
J. W. Allen
J. Barghusen
J. E. Battles
E. C. Berrill
R. L. Breyne
L. Burris
F. A. Cafasso
A. A. Chilenskas
R. Cole
J. G. Eberhart
R. Elliott
B. R. T. Frost
W. Frost
E. C. Gay
A. Gorski
R. Graven
F. Hornstra
R. O. Ivins
R. Kampwirth
G. M. Kesser
R. W. Kessie
V. M. Kolba
M. L. Kyle
W. Lark
S. Lawroski
N. Levitz
L. Link
A. E. Martin
R. G. Matlock
W. R. McIntire
A. Melton
W. E. Miller
F. Mrazek
K. M. Myles
B. Naderer
P. A. Nelson
E. G. Pewitt
A. Rabl
K. Reed
J. J. Roberts
M. F. Roche
R. Rush
W. W. Schertz (266)
V. Sevcik
H. Shimotake
R. K. Steunenberg
C. E. Stevenson
Z. Tomczuk
W. D. Tuohig
D. R. Vissers
S. Vogler
P. Walker
W. J. Walsh
A. Wantroba
D. S. Webster
I. Winsch
R. Winston
R. Yamartino
N. P. Yao
A. B. Krisciunas
ANL Contract File
ANL Libraries (5)
TIS Files (6)

External:

DOE-TIC, for distribution per UC-62 (303)
Manager, Chicago Operations Office
Chief, Office of Patent Counsel, CH
President, Argonne Universities Association
Chemical Engineering Division Review Committee:
- C. B. Alcock, U. Toronto
- R. C. Axtmann, Princeton U.
- R. E. Balzhiser, Electric Power Research Inst.
- J. T. Banchero, U. Notre Dame
- T. Cole, Ford Motor Co.
- P. W. Gilles, U. Kansas
- R. I. Newman, Allied Chemical Corp.
- G. M. Rosenblatt, Pennsylvania State U.

R. W. Allen, U. Maryland
B. N. Anderson, Total Environmental Action, Harrisville, NH
C. Backus, Arizona State U.
M. D. Balcomb, Los Alamos Scientific Laboratory
R. M. Banks, Lawrence Berkeley Lab.
C. S. Barnaby, Berkeley Solar Group
T. R. Beck, Electrochemical Technical Corp., Seattle
W. A. Beckman, U. Wisconsin
J. A. Belding, ET, USDOE
R. F. Boehm, U. Utah
K. W. Boer, U. Delaware
C. E. Bond, U. Illinois, Urbana

P. Bos, Electric Power Research Inst.
P. S. Bringham, Lawrence Berkeley Lab.
H. Buchberg, U. California, Los Angeles
E. Buzzelli, Westinghouse Electric Corp., Pittsburgh
P. Call, Solar Energy Research Inst.
R. Caputo, Altadena, Calif.
I. Catton, U. California, Los Angeles
B. T. Chao, U. Illinois, Urbana
B. Chen, U. Nebraska
W. Christensen, Asst. for Energy Resources, The Pentagon
K. Collier, Los Alamos Scientific Lab.
F. Cornford, Shuron Continental, Rochester
G. Cramer, Southern California Edison, Rosemead
J. E. Cummings, Electric Power Research Inst.
E. S. Davis, Jet Propulsion Lab.
F. DeWinter, Atlas Corp., Santa Clara
J. L. Douglas, Gould Inc., Cleveland
K. Drumheller, Battelle Pacific Northwest Lab.
F. Dubin, DubinMindell-Bloome, Assoc., New York City
W. S. Duff, Colorado State U.
D. K. Edwards, U. California, Los Angeles
J. A. Eibling, Battelle Columbus Lab.
Energy Resources Conservation and Development Commission, Sacramento
R. P. Epple, BES, USDOE
G. Ervin, Rockwell International, Canoga Park
F. Fachat, Kaiser Aluminum & Chemical Corp., Pleasanton
L. T. Fan, Kansas State U.
E. A. Farber, U. Florida
R. L. French, Jet Propulsion Lab.
J. H. B. George, Arthur D. Little, Inc.
S. F. Gilman, State College, Pa.
J. Gough, Motorola, Scottsdale, Ariz.
Y. P. Gupta, E-Systems, Dallas
W. Hassenzahl, Los Alamos Scientific Lab.
H. R. Hay, Skytherm Processors Eng., Los Angeles
H. N. Hersh, Zenith Radio Corp., Chicago
A. F. Hildenbrandt, U. Houston
J. E. Hill, National Bureau of Standards
A. S. Hirshberg, Jet Propulsion Lab.
R. M. Holdredge, Utah State U.
R. Humphries, NASA Marshall Space Flight Center
Dr. Jardine, Colorado Springs, Colo.
P. O. Jarvinen, Masschusetts Institute of Technology
A. Jenkins, Systems, Science and Software
P. E. Jenkins, Texas A&M U.
G. R. Johnson, Colorado State U.
H. Kausman, New York State Energy Research and Development Authority, New York City
W. H. Klein, Smithsonian Institution
J. F. Kreider, Boulder
F. Kreith, Solar Energy Research Inst.
J. Lameiro, Solar Energy Research Inst.
Z. Lavan, Illinois Inst. Technology
G. O. G. Lof, Colorado State U.
D. Ludwig, Intertech Corp., Warrenton, Va.

J. D. MacKenzie, U. California, Los Angeles
C. Mahrok, General Services Adm., Washington
D. K. McDaniels, U. Oregon
J. McKeown, Jr., CS, USDOE
M. Merriam, U. California, Berkeley
A. C. Meyers, Technical Environmental Resources Research Associates, Ames
C. Miller, Chamberlain Mfg. Corp., Waterloo
J. E. Minardi, U. Dayton
D. Moeller, Sun Trac Corp., Wheeling, Ill.
F. H. Morse, U. Maryland
P. W. B. Niles, Calif. Polytechnic State U.
M. C. Noland, Midwest Research Institute
F. Notaro, Union Carbide Corp., Tonawanda
B. A. Phillips, Phillips Engineering Co., St. Joseph
D. R. Reese, Wyle Laboratories, Huntsville
G. T. Reynolds, Princeton U.
R. K. Sakhuja, Thermo Electron Corp. R & D Center, Waltham
A. T. Sales, Georgia Inst. Technology
R. L. San Martin, New Mexico State U.
R. I. Schoen, National Science Foundation
H. J. Schwartz, NASA Lewis Research Center
M. K. Selcuk, Jet Propulsion Laboratory
C. Sepsy, Ohio State U.
A. M. Severson, Minneapolis, Minn.
M. Shell, Thermal Dynamics, Inc., Reston, Va.
B. Shelpuk, RCA Corp., Camden
F. F. Simon, NASA Lewis Research Center
D. L. Spencer, U. Iowa
O. Stephens, General Electric Co., Bellevue, Ohio
E. Streed, National Bureau of Standards
M. Telkes, U. Delaware
G. Thodos, Northwestern U.
E. Thomas, International Silver Co., Meriden
L. Topper, National Science Foundation
U. S. Naval Construction Battalion Center, Port Hueneme
L. Vant-Hull, U. Houston
H. Volkin, Los Alamos Scientific Lab.
M. Wahlig, Lawrence Berkeley Lab.
H. Weinstein, International Rectifier, El Segundo, Calif.
L-C. Wen, Jet Propulsion Lab.
D. H. White, U. Arizona
R. Williams, Georgia Inst. Technology
J. W. Williamson, Vanderbilt U.
M. Wolf, U. Pennsylvania
J. I. Yellot, Arizona State U.
B. L. Youtz, Evergreen State College, Olympia, Wash.
R. Ashby, Ministry of Mining & Natural Resources, Kingston, Jamaica
R. Bruno, Philips Forschungslaboratorium Aachen, Germany
W. W. S. Charters, U. Melbourne, Victoria, Australia
P. I. Cooper, C.S.I.R.O., Victoria, Australia
R. L. Datta, Central Salt and Marine Chemicals Research Inst., Bhavnagar, India
R. V. Dunkle, C.S.I.R.O., Victoria, Australia
J. C. Francken, U. Groningen, The Netherlands
J. T. E. Gilbert, Commission for The Environment, Wellington North, New Zealand

N. K. Gopalkrishnan, Tata Energy Research Inst., Bombay, India
M. C. Gupta, Indian Inst. Technology, Madras, India
S. El-Ein Hedayat, Minister of State for Research and Development, Cairo, Egypt
K. G. Hollands, U. Waterloo, Canada
C. J. Hoogendorn, Technical U. Delft, The Netherlands
R. Kersten, Philips Forschungslaboratorium Aachen GmbH, Aachen, W. Germany
K. Kimura, Waseda University, Tokyo, Japan
V. Korsgaard, Technical U. Denmark, Lyngby
E. Kucys, Lithuanian SSR Academy of Sciences, Vilnius
T. A. Lawland, McGill University, Montreal, Canada
R. N. Morse, C.S.I.R.O., Victoria, Australia
J. Mustoe, London, England
Y. Nakajima, Kojakuin U., Tokyo, Japan
K. S. Ong, U. Malaya, Kuala Lampur, Malaysia
D. Proctor, P.O.B. 26, C.S.I.R.O., Victoria, Australia
D. L. Pulfrey, U. British Columbia, Vancouver, Canada
W. R. Read, C.S.I.R.O., Victoria, Australia
R. Rigopoulos, U. Patras, Greece
A. Roy, U. Negev, P.O.B. 2053, Beer-Sheva, Israel
K. Saito, Osaka Inst. Technology, Osaka, Japan
H. Tabor, The Scientific Research Foundation, Jerusalem, Israel
P. Tiku, Electronics Corp. of India, Hyderabad
F. Trombe, Laboratoire de l'Energie Solaire, Font Romen, France
J. I. B. Wilson, Heriot-Watt U., Edinburgh, Scotland

G. Appleman, Daniel Enterprises, Inc., La Habra, Calif.
M. Doka-Suna, Natural Heating Systems, West Sacramento, Calif.
P. F. Hughes, Science Applications, Inc., McLean, Va.
J. Lowery, Science Applications, Inc., McLean, Va.
K. W. Balk, Kassel, Germany
K. Dehne, Deutscher Wetterdceust, Hamburg, Germany
H. Externest, Bereichsleiter, Bremen, Germany
E. Granryd, Royal Inst. of Technology, Stockholm, Sweden
T. C. Kandpal, Indian Institute of Technology, New Delhi
H. R. Kindra, Bharat Heavy Electricals Ltd., New Delhi, India
R. Kroll, Volkswagenwerk ag Wolfsburg, Wolfsburg, Germany
F. Mahdjuri, Philco Italiana, Bergamo, Italy
A. K. Mohanty, Indian Institute of Technology, Calcutta
S-E. Ransmark, Tekniska Hogskolan, Lund, Sweden
R. Schach, Inst. für Elektrische Maschinen, Berlin, Germany
L. Schmieder, Gilching, Germany
K. R. Schreitmüller, Institut für Technische Physik, Stuttgart, Germany
S. D. Verma, Gujarat University, Ahmedabad, India